

Article

New Biochronological Scales of Planktic Foraminifera for the Early Danian Based on High-Resolution Biostratigraphy

Ignacio Arenillas ^{*}, Vicente Gilabert and José A. Arz 

Departamento de Ciencias de la Tierra, Instituto Universitario de Investigación en Ciencias Ambientales de Aragón (IUCA), Universidad de Zaragoza, E-50009 Zaragoza, Spain; vgilabert@unizar.es (V.G.); josearz@unizar.es (J.A.A.)

* Correspondence: ias@unizar.es

Abstract: After the Cretaceous/Paleogene boundary (KPB) catastrophic mass extinction event, an explosive evolutionary radiation of planktic foraminifera took place in consequence of the prompt occupation of empty niches. The rapid evolution of new species makes it possible to establish high-resolution biozonations in the lower Danian. We propose two biostratigraphic scales for low-to-middle latitudes spanning the first two million years of the Danian. The first is based on qualitative data and includes four biozones: the *Guembelitra cretacea* Zone (Dan1), the *Parvularugoglobigerina longiapertura* Zone (Dan2), the *Parvularugoglobigerina eugubina* Zone (Dan3), and the *Parasubbotina pseudobulloides* Zone (Dan4). The latter two are divided into several sub-biozones: the *Parvularugoglobigerina sabina* Subzone (Dan3a) and the *Eoglobigerina simplicissima* Subzone (Dan3b) for the *Pv. eugubina* Zone, and the *Praemurica taurica* Subzone (Dan4a), the *Subbotina triloculinoides* Subzone (Dan4b), and the *Globanomalina compressa* Subzone (Dan4c) for the *P. pseudobulloides* Zone. The second scale is based on quantitative data and includes three acme-zones (abundance zones): the *Guembelitra* Acme-zone (DanAZ1), the *Parvularugoglobigerina-Palaeoglobigerina* Acme-zone (DanAZ2), and the *Woodringina-Chiloguembelina* Acme-zone (DanAZ3). Both biozonations are based on high-resolution samplings of the most continuous sections of the lower Danian worldwide and have been calibrated with recent magnetostratigraphic and astrochronological dating.

Keywords: planktic foraminiferal biozonation; acme-zonation; biochronology; lower Danian; magnetostratigraphic-astronomical calibration



Citation: Arenillas, I.; Gilabert, V.; Arz, J.A. New Biochronological Scales of Planktic Foraminifera for the Early Danian Based on High-Resolution Biostratigraphy. *Geosciences* **2021**, *11*, 479. <https://doi.org/10.3390/geosciences11110479>

Academic Editors: Maria Rose Petrizzo, Lucilla Capotondi, Angela Cloke-Hayes and Jesus Martinez-Frias

Received: 30 August 2021
Accepted: 18 November 2021
Published: 22 November 2021

Publisher's Note: MDPI stays neutral with regard to jurisdictional claims in published maps and institutional affiliations.



Copyright: © 2021 by the authors. Licensee MDPI, Basel, Switzerland. This article is an open access article distributed under the terms and conditions of the Creative Commons Attribution (CC BY) license (<https://creativecommons.org/licenses/by/4.0/>).

1. Introduction

The high biostratigraphic resolution of planktic foraminifera is a result of their rapid evolution. The first and last appearances of planktic foraminiferal species occur within a relatively short period of geological time, usually providing us with detailed biochronological records [1,2]. A large number of biostratigraphic horizons (biohorizons) can be recognized, but not all of them are of any utility in biostratigraphy and biochronology. Only a few species, the so-called index species, allow robust biostratigraphic correlation, due to their easy taxonomic distinction, high abundance, short chronological and stratigraphic distribution, wide biogeographic distribution, and high preservation potential. The lowest and highest occurrence data (LOD and HOD) of index species are the most widely used key-biohorizons for defining planktic foraminiferal biozones and sub-biozones, these being mainly of two kinds: range zones (with two subtypes: taxon-range and concurrent-range zones) and interval zones (with three subtypes: lowest-occurrence, highest-occurrence, and partial-range zones). Other kinds of biozone, such as abundance zones (acme-zones), are not commonly used for planktic foraminiferal zonations.

The highest resolution of the planktic foraminiferal biostratigraphic scales is achieved in the lower Danian, after the Cretaceous/Paleogene boundary (KPB) mass extinction, because numerous small-size species began to appear following a model of “explosive” evolutionary radiation [3,4]. Planktic foraminiferal specialists have tended to establish

increasingly detailed biozonations for the lower Danian in order to analyze in ever greater detail the succession, time, and duration of the rapid paleobiological, paleoenvironmental and paleoclimatic changes that occurred after the KPB, which are currently the subject of intensive study [5–9].

In 1957, the *Globorotalia trinidadensis* Zone was considered the stratigraphically lowest biozone of the Danian because it overlaid the Cretaceous sequence in Trinidad [1]. Around the same time, the *Globigerina trivialis* Zone [10] and the *Globigerina pseudobulloides*–*Globigerina daubjergensis* Zone [11] were recognized in the Caucasus at lower stratigraphic levels; these were eventually renamed the *Globigerina pseudobulloides* Zone [12] and called Biozone P1 in the system of alphanumeric nomenclature [13,14].

More precise biostratigraphic studies in Gubbio (Italy) revealed in 1964 that below the *Globigerina pseudobulloides* Zone there was a new planktic foraminiferal assemblage of tiny trochospiral species, later called parvularugoglobigerinids, allowing the so-called *Globigerina eugubina* Zone, or Biozone P α in the alphanumeric nomenclature [15], to be defined [3,12,16,17]. Finally, in 1982, high-resolution biostratigraphic studies in Caravaca (Spain) allowed a very thin biostratigraphic interval to be recognized between the KPB mass extinction and the LOD of incoming Danian species (parvularugoglobigerinids), which was called the *Guembelitra cretacea* Zone or Biozone P0 [4]. Since then, the standard biozones have been subdivided into different subbiozones in the new lowermost Danian biostratigraphic scales [2,18–26], reaching a very high degree of resolution.

None of the planktic foraminiferal zonations defined for the lower Danian are completely free of taxonomic problems. Several planktic foraminiferal taxonomies have been proposed for the early Danian [3,15,16,27–29]. These differ both in the taxonomic identification of some index species and in the suggested biochronostratigraphic ranges, causing some inconsistencies among the planktic foraminiferal biozonations, which are addressed in this paper.

Having conducted a review of ten selected lower Danian sections, which are among the most expanded, complete, and continuous sections in Spain, Tunisia, Mexico, and Cuba, we propose two alternative planktic foraminiferal zonations for the lower Danian, applicable for low and middle latitudes of the Northern Hemisphere, and oceanic and outer neritic environments: one based on updated qualitative data and stratigraphic ranges (interval zones), and the other based on quantitative data (abundance zones or acme-zones). The former is correlated with the most standardized biozonations and calibrated with recent high-resolution magnetostratigraphical and astrochronological dating. The latter allows potential taxonomic problems to be minimized and makes it easier to establish the biochronostratigraphic range of index species and the emplacement of the boundaries between interval zones.

2. Reference Sections, Key Biohorizons, and Calibration Methods

The two lower Danian biozonations proposed here are mainly based on the pelagic sections of Caravaca [8,24,30–32], Zumaia [9,24,30,33] and Agost [24,34] (Spain), Gubbio [9,35,36] (Italy), El Kef [24,37–40], Ain Settara [24,30,39,41,42] and Elles [24,30,43] (Tunisia), La Lajilla [24,44] and Bochil [30,45] (Mexico), and Moncada [46] (Cuba) (Figure 1), which we studied preferably with high-resolution methodology. This selection includes the El Kef section, where the Global Boundary Stratotype Section and Point (GSSP) for the base of the Danian Stage was defined [37], and most of the designated auxiliary sections (Caravaca, Zumaia, Ain Settara, Elles, and Bochil) [30]. The paleodepth of most of these reference sections are summarized in Molina et al. [30,37] and Schulte et al. [47]: the sections span paleodepths from outer sublittoral (El Kef, Ain Settara and Elles) to bathyal (Caravaca, Zumaia, Agost, Gubbio, La Lajilla, Bochil, and Moncada). The biostratigraphic ranges of the planktic foraminiferal species shown in Figure 2, and the changes in relative abundance of planktic foraminiferal groups across the lower Danian shown in Figure 3, are the result of a review, compilation, and correlation of stratigraphic studies carried out by us at all these localities. The state of preservation of the planktic foraminifera in the reference

sections varies from very good (as in the El Kef section) to poor (as in the Moncada section), but in all cases are well enough preserved to permit rigorous taxonomic identification and consistent biostratigraphic and quantitative studies.

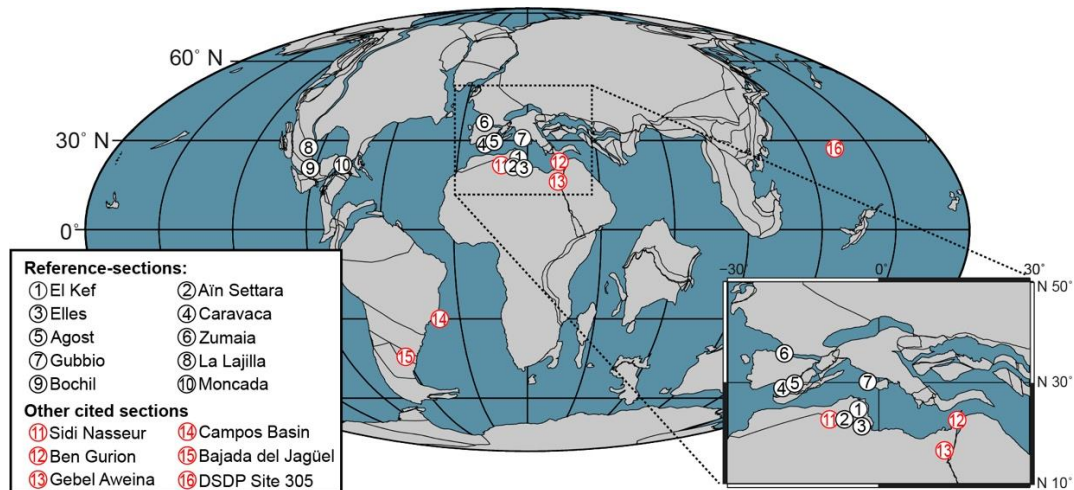


Figure 1. Paleogeographic reconstruction for the KPB (66 Ma), with the localities cited in this study (after https://www.odsns.de/odsns/services/paleomap/adv_map.html (accessed on 3 July 2021)).

The planktic foraminiferal key-biohorizons of the qualitative biozonation proposed here are the same as those used by Arenillas et al. in a previous biozonation [24]: i.e., the KPB mass extinction horizon (or the HOD of *Abathomphalus mayaroensis*), and the LODs of *Parvularugoglobigerina longiapertura*, *Parvularugoglobigerina eugubina*, *Eoglobigerina simplicissima*, *Parasubbotina pseudobulloides*, *Subbotina triloculinoides*, and *Globanomalina compressa*. The key biohorizons of the proposed acme-zonation are the same as those used by Arenillas et al. [45] in defining the Planktic Foraminiferal Acme Stages (PFAS): i.e., the LODs of the *Guembeltria* acme (PFAS-1), the *Parvularugoglobigerina-Palaeoglobigerina* acme (PFAS-2), and the *Woodringina-Chiloguembelina* acme (PFAS-3). Here, we provide updated magnetostratigraphical and astronomical calibrations (in kyr after the KPB) of all these key-biohorizons and an average estimate of the ages (in Ma) of the base and top of the proposed biozones.

For the magnetostratigraphical calibrations, we rely on a recent bio-magnetostratigraphical correlation from the Caravaca section performed by Gilabert et al. [8] (see details in Supplementary Table S1). The lowermost Danian at Caravaca is characterized by a ~6 cm thick dark clay bed, with a ~2 cm thick darker clay in its basal part [4,30,48]. The base of this dark clay marks the KPB, and consists of a 1 to 2 mm thick red airfall layer containing high concentrations of iridium and impact ejecta, such as altered glass spherules, Ni-spinels, shocked quartz, etc. [4,49–52]. This level coincides with the planktic foraminiferal mass extinction horizon [4,31,34,53].

To establish the age model at Caravaca, we linearly interpolate between the KPB, the top of the KPB dark clay bed, and the C29r/C29n, C29n/C28r, C28r/C28n, and C28n/C27r magnetic reversals. Following the Geological Time Scale 2020 [54] for the early Danian, which is based on astronomical calibrations [55], we assign an age of 66.001 Ma to the KPB, 65.700 Ma to the C29r/C29n reversal, 64.862 Ma to C29n/C28r, 64.645 Ma to C28r/C28n, and 63.537 Ma to C28n/C27r: i.e., 0, 301, 1139, 1356 and 2464 kyr after the KPB, respectively (Table 1).

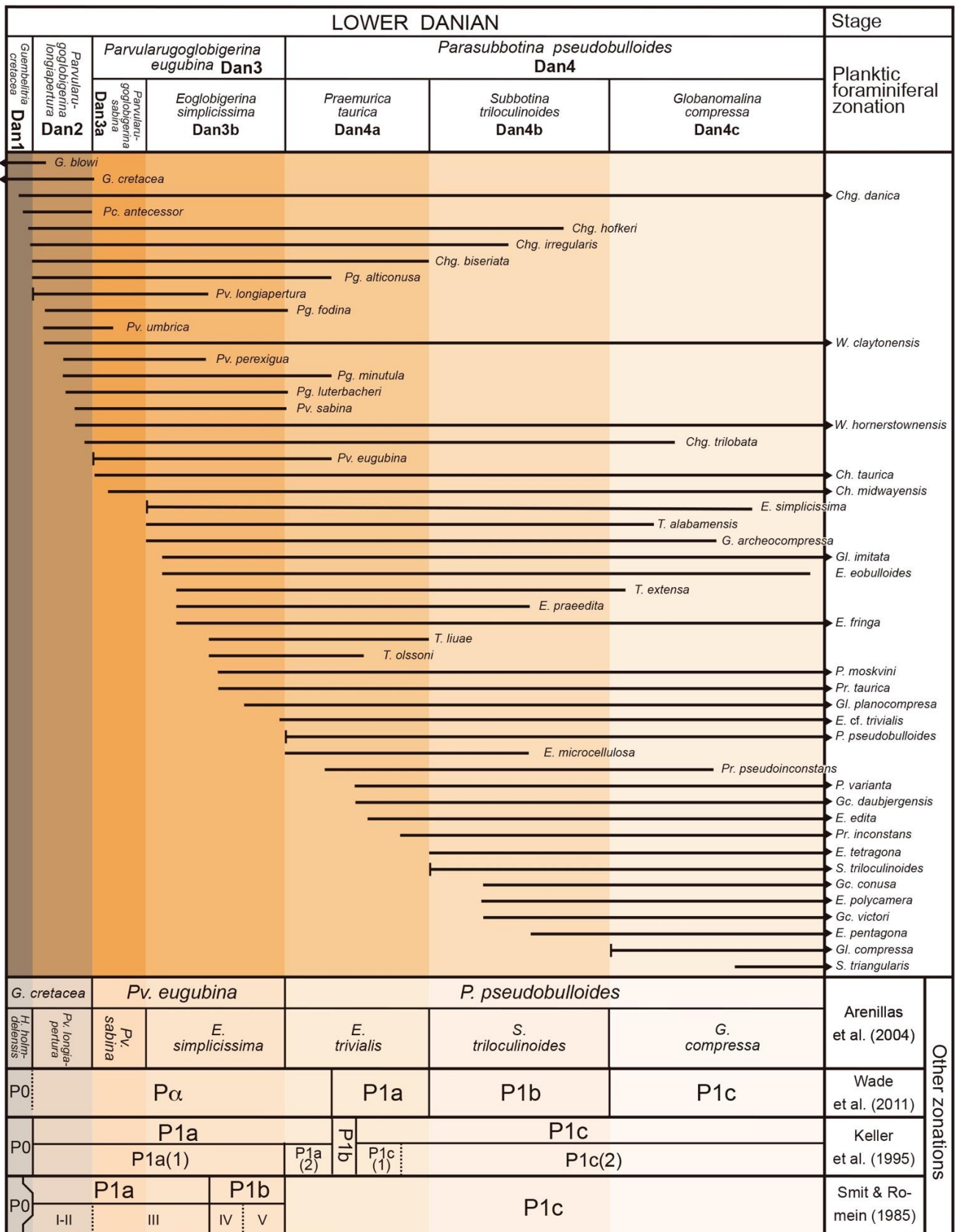


Figure 2. Qualitative biozonation proposed in this paper, and biostratigraphic ranges of early Danian planktic foraminiferal species based on high-resolution biostratigraphic studies (see references in text). Comparison with the most widely used P-biozonations: (1) Arenillas et al. [24]; (2) Wade et al. [2]; (3) Keller et al. [23]; (4) Smit and Romein [18].

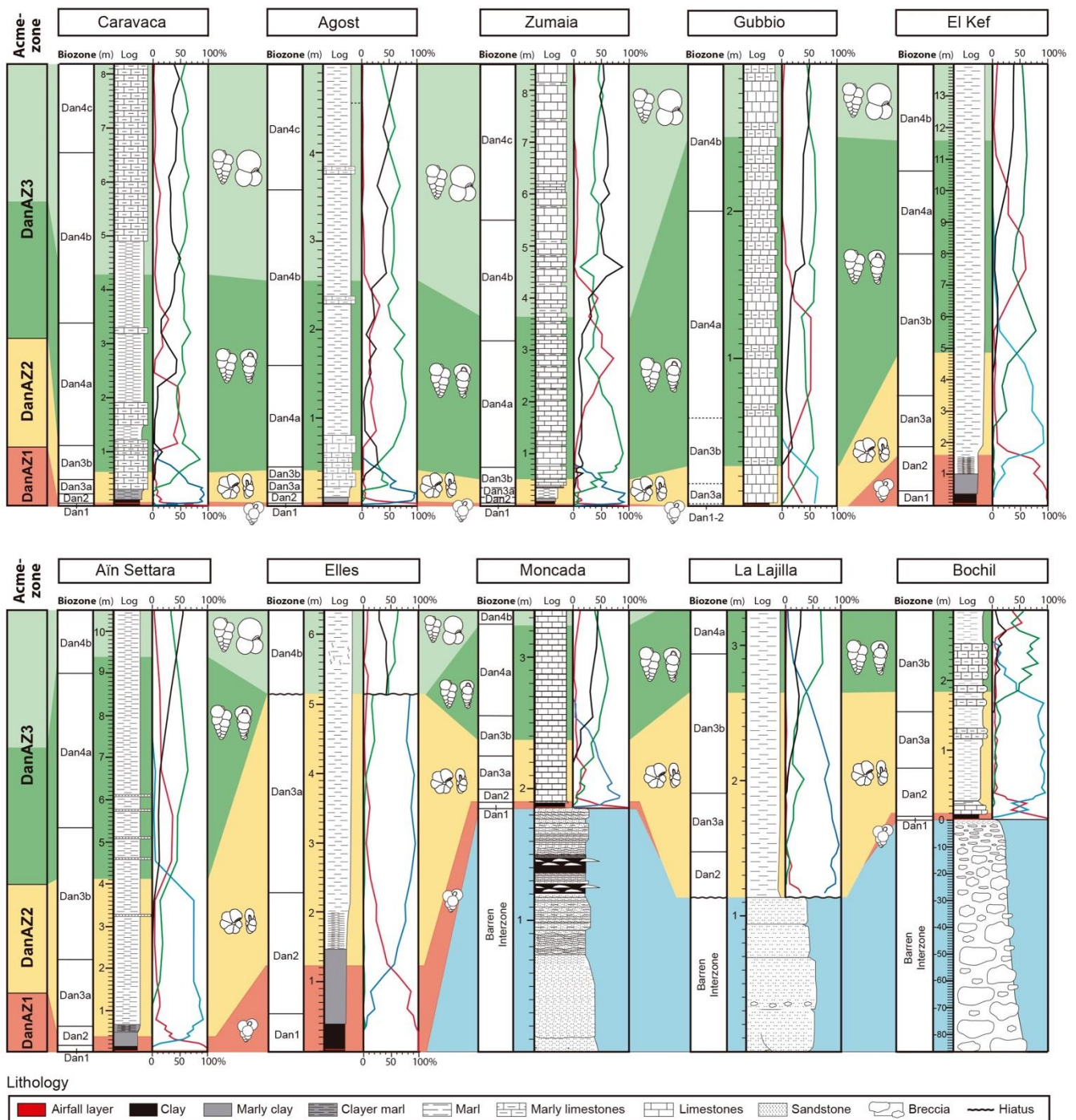


Figure 3. Planktic foraminiferal acme-zonation proposed in this report, and relative abundance of planktic foraminiferal groups across the lower Danian at the reference sections: Caravaca (middle bathyal; Spain) [8], Agost (upper-middle bathyal; Spain) [34], Zumaia (middle bathyal; Spain) [9], Gubbio (lower bathyal; Italy) [9], El Kef (outer sublittoral-upper bathyal; Tunisia) [40], Ain Settara (outer sublittoral; Tunisia) [41], Elles (outer sublittoral; Tunisia) [43], Moncada (upper bathyal; Cuba) [46], La Lajilla (lower bathyal; Mexico) [44], and Bochil (upper bathyal; Mexico) [45]. Red line = triserial guembelitrIID group (*Guembelitra* and *Chiloguembelitra*). Blue line = smooth-walled parvularugoglobigerinid group (*Parvularugoglobigerina*, *Palaeoglobigerina* and *Pseudocaucasina*). Green line = biserial group (*Woodringina* and *Chiloguembelina*). Black line = other genera (*Eoglobigerina*, *Globanomalina*, *Parasubbotina*, *Praemurica*, *Subbotina*, *Trochoguembelitra*, and *Globoconusa*). For Acme-zone DanAZ3, dark green shading: dominance of *Woodringina-Chiloguembelina*, and light green shading: codominance of *Woodringina-Chiloguembelina* and other genera (*Eoglobigerina-Subbotina-Parasubbotina-Globanomalina-Praemurica*).

Since the estimated duration for the deposition of the KPB dark clay bed is ~10 kyr, based on cosmic ^3He sedimentation rates [56], the top of the KPB dark clay bed is calibrated at 65.991 Ma. The stratigraphic positions of the magnetozones at Caravaca (Table 1) are based on those reported by Smit [4] and Groot et al. [57]. At Caravaca, the C29r/C29n, C29n/C28r, C28r/C28n, and C28n/C27r magnetic reversals are 5.1, 9.8, 12.3, and 20.3 m above the KPB. Consequently, the average sedimentation rates at Caravaca are 0.60 cm/kyr for the KPB dark clay bed, 1.67 cm/kyr for the Danian part of C29r, 0.41 cm/kyr for C29n, 0.18 cm/kyr for C28r, and 0.30 cm/kyr for C28n.

Table 1. Data for magnetostratigraphical and astronomical calibrations in the Caravaca and Zumaia reference-sections. Stratigraphic position (cm from the KPB) of tie-points, and their calibrated ages (in Ma and kyr after the KPB) according to GTS 2020 [54].

Tie Points (Key-Horizons)	Section	Height cm from KPB	GTS2020 Ma	kyr after KPB
KPB	Caravaca	0	66.001	0
KPB dark clay bed top	Caravaca	6	65.991	10
C29r/C29n reversal	Caravaca	510	65.700	301
C29n/C28r reversal	Caravaca	980	64.862	1139
C28r/C28n reversal	Caravaca	1230	64.645	1356
C28n/C27r reversal	Caravaca	2030	63.537	2464
KPB	Zumaia	0	66.001	0
KPB dark clay bed top	Zumaia	9	65.991	10
405-kyr min.	Zumaia	50	65.967	34
405-kyr max. Pc ₄₀₅ 1	Zumaia	365	65.760	241
405-kyr min.	Zumaia	615	65.555	446
405-kyr max. Pc ₄₀₅ 2	Zumaia	865	65.353	648

For the astrochronological or astronomical calibrations, we rely on new high-resolution biostratigraphic and cyclostratigraphic studies by Gilabert et al. [9] on the Zumaia section (see details in Supplementary Table S2). The lowermost Danian at Zumaia is characterized by a ~9 cm thick dark clay bed, with a ~2 cm thick darker clay in its basal part, and a 1 to 2 mm thick airfall layer at its base containing the KPB impact material [9,58–60]. Due to its exceptional exposure and the rhythmic alternation of carbonate-rich and carbonate-poor lithologies, several cyclostratigraphic analyses have made it possible to establish astronomically calibrated age models at Zumaia [55,61–68]. Gilabert et al. recently correlated the stable 405 kyr long, eccentricity-modulated precession cycles in the 1 Myr interval across the KPB [9], connecting previous well-resolved cyclostratigraphic studies of the Maastrichtian [67] and Danian [55]. The tie-points (key-horizons) for age calibration are the 405 kyr eccentricity maxima and minima extracted from the La2011 astronomical solution [69], and a KPB age of 66.001 Ma [54,55]. This age for the KPB differs from recent U-Pb and $^{40}\text{Ar}/^{39}\text{Ar}$ dating efforts, which yielded results of 66.016 ± 0.05 Ma [70] and $66.052 \pm 0.008/0.043$ Ma [71] respectively, but it falls within the uncertainties of these estimates. Calibrated ages by Gilabert et al. [9] were linearly interpolated within each precession cycle recognized between the above-cited tie-points, allowing the large, orbitally driven changes in the sedimentation rate at the Zumaia section to be accounted for, and providing a detailed age calibration of the key-biohorizons (Table 1).

3. Taxonomic Notes

The planktic foraminiferal taxonomy used here (Figures A1–A5; Supplementary Text S1) as a basis for determining the biostratigraphic ranges of the species in Figure 2 is based on detailed morphological-ontogenetic analysis and high-resolution biostratigraphic studies mainly performed in Tunisian sections, such as El Kef [24,37–40]. This taxonomy differs partially from the one most used by lower Danian biostratigraphers [29], both in the number of species distinguished and in the diagnostic criteria for differentiating some of the species: for example, the most widespread taxonomy [29] assigns the morphological characters

of all species of *Guembelitra* and *Chiloguembelitra* (Figure A1) to only one: *Guembelitra cretacea*.

Similar differences occur when distinguishing species in *Parvularugoglobigerina* (Figures A2 and A3; Supplementary Text S1), among which Olsson et al. [29] only consider three species (*Pv. eugubina*, *Pv. alabamensis*, and *Pv. extensa*); in *Eoglobigerina* (Figure A4), among which they only consider two species (*E. eobulloides* and *E. edita*); and in *Globanomalina* (Figure A5), among which they only consider three species (*Gl. archeocompressa*, *Gl. planocompressa*, and *Gl. compressa*). The different taxonomic criteria used among early Danian planktic foraminiferal specialists cause apparent differences in the stratigraphical distribution of some index species (see discussion below), and effectively compromise the rigor of the biochronological scales.

In order to provide a clearer exposition of the taxonomy followed here, we summarize in Figures A1–A5 and Supplementary Text S1 the morphological and textural criteria used to distinguish the early Danian planktic foraminiferal species and genera, and illustrate specimens of each of them, which were photographed under a Zeiss MERLIN FE-SEM at the Universidad de Zaragoza (Spain). The planktic foraminiferal specimens are from El Kef, Ain Settara, and Sidi Nasseur (Tunisia), Gebel Aweina (Egypt), Ben Gurion (Israel), Bajada del Jagüel (Argentina), and DSDP Site 305 (Shatsky Rise, northwestern Pacific). In Figure A1, note that *Chiloguembelitra* exhibits a microperforate rugose and/or pustulate rugose wall texture, unlike *Guembelitra*, which displays a typical pore-mounded wall texture. In Figure A3, note that specimens of *Parvularugoglobigerina* and other parvularugoglobigerinids (*Pseudocaucasina* and *Palaeoglobigerina*) exhibit a smooth wall texture when well preserved, but a rough or microgranular wall surface when their surface is recrystallized. This contrasts with the wall texture of *Trochoguembelitra* (Figure A2), which is similar to that of *Chiloguembelitra*. Note that the diagnostic characters of the genus *Trochoguembelitra* were assigned by Olsson et al. [29] to *Parvularugoglobigerina*. In Figure A5; note also that specimens of *Acarinina trinidadensis* and *Acarinina uncinata* exhibit a muricate wall texture when well preserved, unlike the *Praemurica* species.

4. Some Thoughts on the Lower Danian Planktic Foraminiferal Zonations

4.1. Parallel Nomenclature in Qualitative Biozonations Based on Ranges of Index Species

The first planktic foraminiferal zonations in the 1950s and 1960s for the lower Danian used the conventional system of binomial nomenclature in naming biozones: i.e., using the name/s of index species employed to define them [1,2,10,11]. The use of a system of alphanumeric nomenclature, i.e., sequentially numbering biozones, became widespread in the 1970s [13–15]. Biozones with an alphanumeric nomenclature feature the disadvantage of being very inflexible and, once published, they do not lend themselves easily to the insertion of new biozones or the elimination of old ones, as these alter the order and create confusion. The same alphanumeric designation can be used in a different sense by biostratigraphers, creating added confusion. The fundamental reason is that these biozone names lack intrinsic meaning and provide very little information on the micropaleontological content.

This problem is especially relevant for the lower Danian, as at least four different alphanumeric biozonations using the “P” notation have been proposed [2,15,18,23], which is very confusing for non-specialists. However, this system provides biostratigraphers with a useful and easy mnemonic means of communication, because it automatically indicates the order and relative position of the biozones and is advantageous in both written and verbal presentation. For this reason, a combined binomial and alphanumeric nomenclature system is sufficient to resolve doubts about the alphanumeric designations.

To avoid confusion with the P-notation of previous biozonations [2,15,18,23], we here propose a new alphanumeric notation (“Dan”) for the Danian biozones. Figure 2 includes a comparison of this new qualitative Dan-biozonation with the most standardized P-biozonation [2] as well as with others that have also been frequently used [18,23,24].

4.2. Inconsistencies in Qualitative Biozonations Due to Taxonomic Discrepancies

One of the main taxonomic problems in biostratigraphy is the discord between splitter and lumper taxonomists. Discrepancies over recognizing few or many species are caused by the difficulty of distinguishing “real” biological species in the micropaleontological record in the face of traditional morphological analyses (biospecies vs. morphospecies concepts). There are arguments for and against both positions. However, in practice, the species ranges proposed by two biostratigraphers cannot be accurately compared or correlated if there are taxonomic discrepancies between them, creating confusion among non-specialists.

In the lowermost Danian, the most obvious case of the divergence between splitter and lumper taxonomies is exemplified by the genus *Parvularugoglobigerina* [5,29,38]. According to the planktic foraminiferal taxonomy most frequently used by lower Danian biostratigraphers [29], *Parvularugoglobigerina* comprises only three species (*Pv. eugubina*, *Pv. alabamensis*, and *Pv. extensa*), with both pore-mounded and smooth wall textures. The more splitter-oriented taxonomy used here proposes up to four different genera for these morphologies: *Parvularugoglobigerina*, *Palaeoglobigerina*, *Pseudocaucasina*, and *Trochoguembelitra*, and a total of fourteen species (Figures A2 and A3). Failure to recognize the latter three genera and their species may have led some biostratigraphers to claim that the LODs of species of *Globanomalina*, *Eoglobigerina*, *Praemurica*, and *Globoconusa* are in Biozone P0 or close to the P0/P α Biozone boundary [5,23,25,29,72].

Other taxonomic discrepancies arise in species delimitation within lineages that have evolved gradually (i.e., chronospecies delimitation in anagenetic evolutionary lineages). On many occasions, this leads taxonomists and biostratigraphers to place the first appearance of a given species at different times [2,7,24], resulting in apparent diachronism in key-biohorizons. This may be the source of discrepancies in the biochronostratigraphic position of index species such as *S. triloculinoides*⁽¹⁾, *Gl. compressa*⁽²⁾, and *A. trinidadensis*⁽³⁾. These belong to three anagenetic lineages: ⁽¹⁾ *Eoglobigerina simplicissima* → *E. microcellulosa* → *Subbotina triloculinoides* → *S. triangularis*; ⁽²⁾ *Globanomalina archeocompressa* → *Gl. planocompressa* → *Gl. compressa* → *Gl. haunsbergensis* → *Luterbacheria ehrenbergi*; and ⁽³⁾ *Praemurica taurica* → *Pr. pseudoinconstans* → *Pr. inconstans* → *Acarinina trinidadensis* → *Ac. uncinata* (Figures A4 and A5), where the boundaries between species are not precise, giving rise to subjective delimitations [17,35].

4.3. Acme-Zonation (Quantitative Biozonation) as an Alternative

Since taxonomic discrepancies and subjectivity can greatly influence biostratigraphic studies, it is necessary to find an alternative that offers more objective criteria, even if this causes a loss of biostratigraphic resolution. For the lower Danian, this alternative is provided by quantitative data and the establishment of an acme-zonation (Figure 3). An abundance zone or acme-zone represents the interval of maximum apogee (acme), generally the maximum relative abundance, of a particular taxon or taxon set. The boundaries of an abundance zone are defined by the biohorizons at which there is a notable change in the abundance of the index taxon or taxa (key-acme-horizons): a rapid increase for the base and a rapid decrease for the top. The acme zone takes its name from the most significant or abundant index taxon or taxa. For the definition of acme zones, it is convenient to analyze the samples quantitatively to locate their base and top with greater precision.

The use of quantitative data, especially when referring to the relative abundances of a species set (e.g., a genus or a genus set), minimizes the subjectivity and confusion present in the taxonomic determination of a particular species. Two biostratigraphers or two taxonomists may disagree when identifying a species due to their divergent preferences for splitter or lumper taxonomies or simply due to their assignation of different names. However, they are more likely to agree when identifying the acme of a species set characterized by easy-to-distinguish morphologies. For example, in the lower Danian, it is easier to agree over the recognition of an acme of parvularugoglobigerinids than in the taxonomic identification of *Pv. eugubina*.

A previous step in defining abundance zones is the identification of quantitative intervals or acme stages, delimited by two key acme horizons (base and top). An acme stage is an informal biostratigraphic unit that refers to each of the quantitative intervals or episodes recognizable in the stratigraphic record. To define an abundance zone, it is necessary first to trace it laterally, i.e., to check that the acme stage is useful for biochronostratigraphic correlation. An unusual relative abundance of a particular taxon or taxa in the stratigraphic record may result from a number of processes that can be local, diachronic in different localities, or repeated in different times. Acme stages with these characteristics can be useful to define ecozones, which are the minimum ecostratigraphic units characterized by shifts in type assemblages linked to paleoenvironmental changes. Their utility for correlation is normally local or regional, although it can also be global if paleoenvironmental changes are triggered by eustatic and climatic cycles (Milankovitch cycles). However, there are some acme stages linked to evolutionary processes, and these consequently do not repeat in time. If its lateral traceability or biochronostratigraphic utility is demonstrated, the identification of an acme stage may allow an abundance zone to be formally defined. Like any other biostratigraphic unit, the base of an acme zone must be based on the stratigraphic record of a bioevent that does not repeat in time.

In the lower Danian, several distinctive acme stages have been recognized [33,40,41], allowing the so-called PFASs to be identified [45]: PFAS-1 (dominance of triserial species of the genus *Guembelitra*), PFAS-2 (dominance of tiny trochospiral species of the genera *Parvularugoglobigerina* and *Palaeoglobigerina*), and PFAS-3 (dominance or high abundance of biserial species of the genera *Woodringina* and *Chiloguembelina*). The PFASs, which are the basis for the acme-zonation proposed here, were established after quantitative studies carried out on the >63 μm size-fraction [33,40,41,45]. This acme zonation also appears to be valid for studies carried out on <63 μm size-fractions [73,74], but the synchronicity of acme horizons recognized in these size fractions should be better contrasted. These acme-stages have been identified worldwide (Figure 3), mainly in the Tethys, North Atlantic, Gulf of Mexico, and Caribbean [6,8,9,42,45,46,72,74,75] but also in the Central Pacific and South Atlantic [9,18,76], suggesting that they are useful for global stratigraphic correlation. The succession of acme stages and their synchronicity seems to be independent of the heterogeneous conditions of ocean productivity after the KPB extinction event [6,8,9,74], at least in the localities and environments where these acme stages have been recognized and analyzed by us.

5. Calibration of Key-Biohorizons

Figure 4 and Tables 1 and 2 summarize the age model and magnetostratigraphic calibrations of key biohorizons in the Caravaca reference section, which are based on GTS 2020 [54] and a bio-magnetostratigraphic correlation [8,35]. Details of the magnetostratigraphic calibration of the bases of the biozones and acme zones are shown in Supplementary Table S1. At Caravaca, the LODs of *Pv. longiapertura*, *Pv. eugubina*, *E. simplicissima*, *P. pseudobulloides*, *S. triloculinoides*, and *Gl. compressa* are respectively placed 3, 22, 42, 107, 332, and 655 cm above the KPB (Table 2). According to the age model at Caravaca, these key-biohorizons are bio-magnetostratigraphically calibrated 5, 19, 31, 68, 198, and 560 kyr after the KPB, respectively (Figure 4). In addition, the LODs of the *Parvularugoglobigerina*-*Palaeoglobigerina* and *Woodringina*-*Chiloguembelina* acmes are respectively placed 5 and 55 cm above the KPB and are calibrated 8 and 38 kyr after the KPB, respectively (Figure 4).

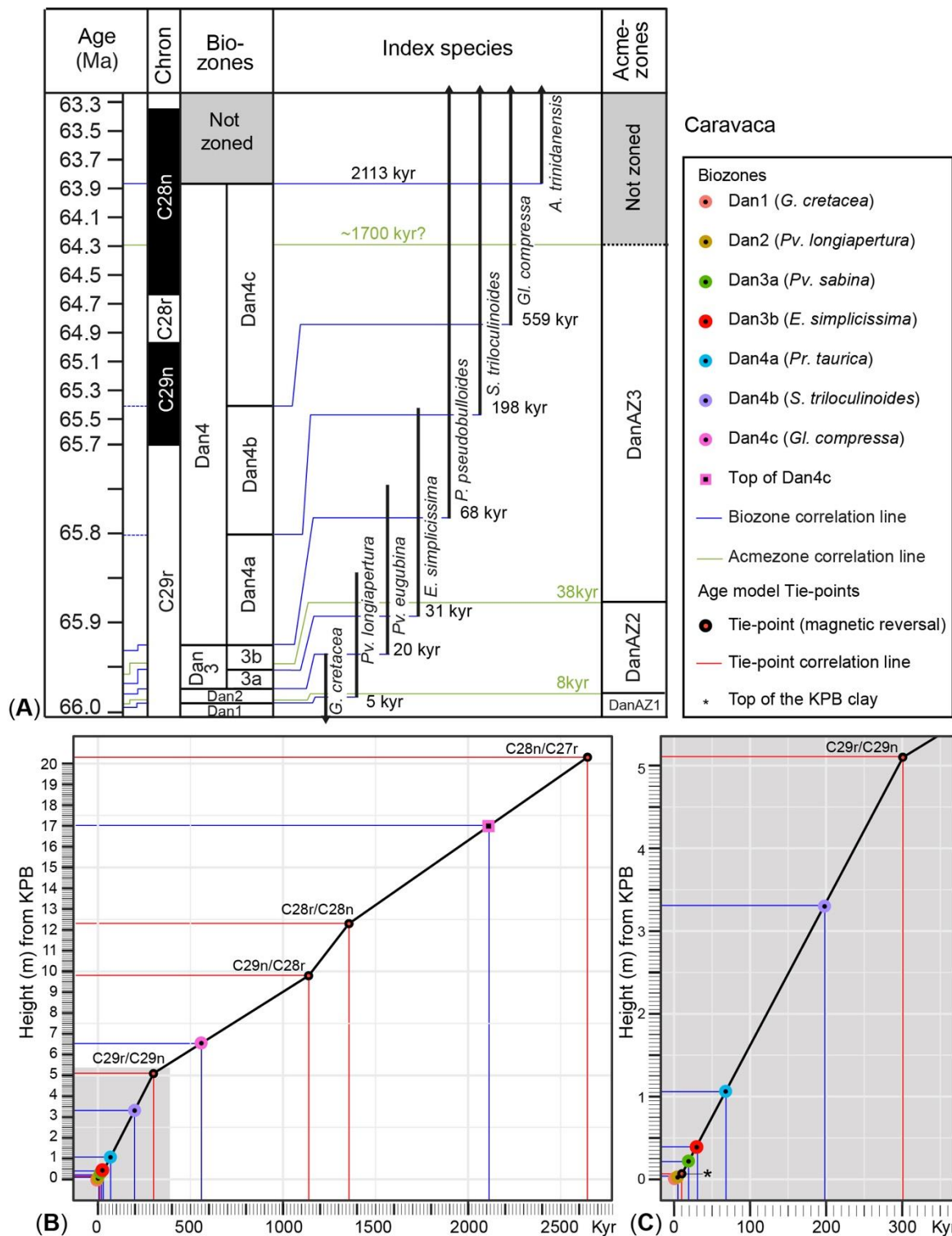


Figure 4. Magnetostratigraphical calibration of the bases of the biozones and acme zones proposed in this report, based on GTS 2020 [54] and the bio-magnetostratigraphic correlation in the Caravaca reference section [8,35]; (A)—bio-magnetostratigraphical correlation and magnetostratigraphically calibrated ages of key biohorizons; (B,C)—Graphic correlations to establish the age model at Caravaca, using as tie-points (key-horizons) the KPB, the top of the KPB dark clay bed, and the magnetic reversals.

Figure 5 and Tables 1 and 2 summarize the age model and astronomical calibrations of key biohorizons in the Zumaia reference section, which are based on the La2011 astronomical solution [69] and a bio-cyclostratigraphic correlation [9]. Details of the astronomical calibration of the bases of the biozones and acme zones are shown in Supplementary Table S2. At Zumaia, the LODs of *Pv. longiapertura*, *Pv. eugubina*, *E. simplicissima*, *P. pseudobulloides*, *S. triloculinooides*, and *Gl. compressa* are placed 6, 23, 37, 100, 330, and 655 cm above the KPB (Table 2). According to the orbital tuning at Zumaia, these key-biohorizons are astronomically calibrated 7, 18, 26, 68, 210, and 473 kyr after the KPB, respectively (Figure 5). In addition, the LODs of the *Paroularugoglobigerina*-*Palaeoglobigerina* and *Woodringina*-*Chiloguembelina* acmes are placed 6 and 55 cm above the KPB and are calibrated 7 and 42 kyr after the KPB, respectively (Figure 5).

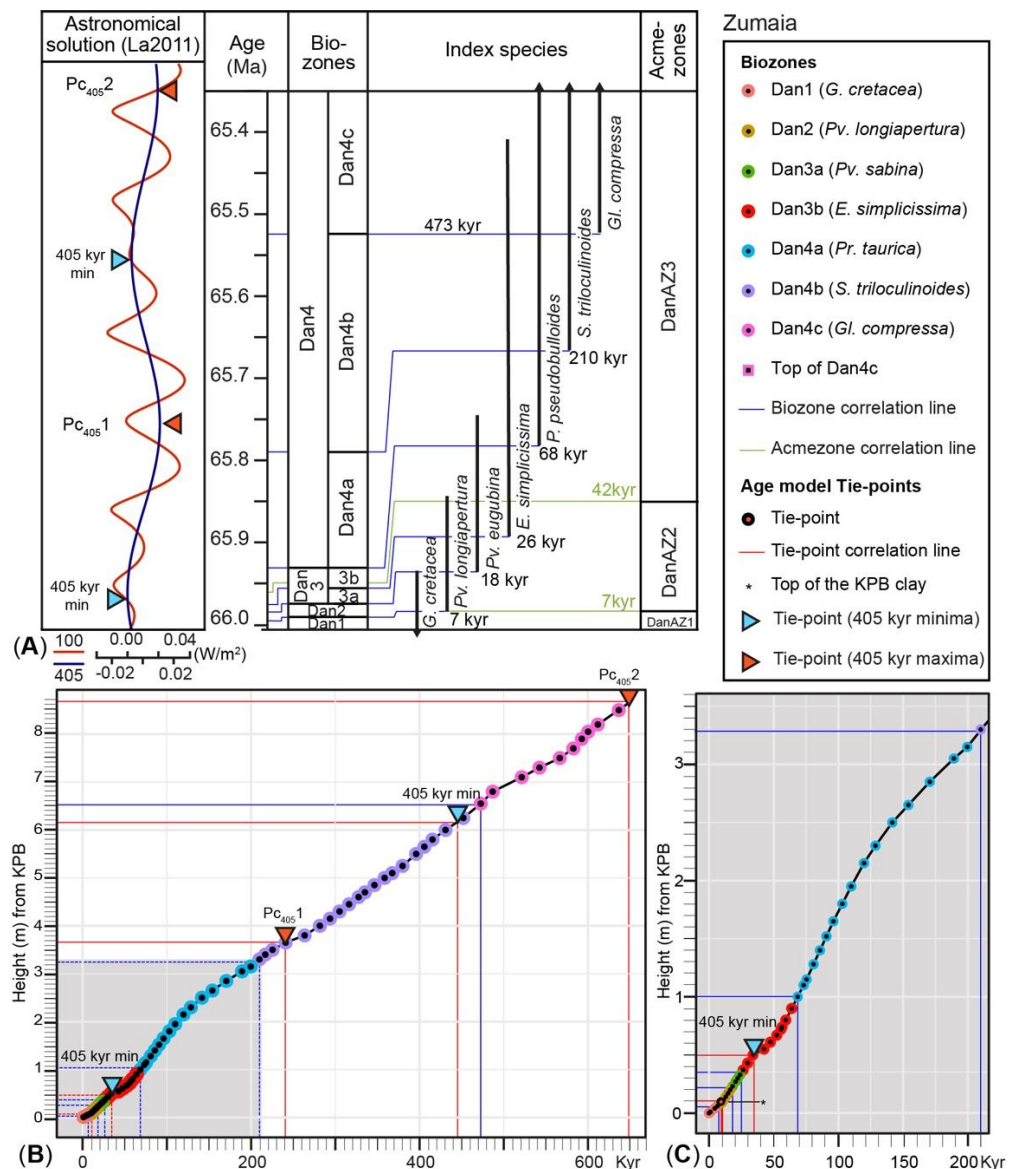


Figure 5. Astronomical calibration of the bases of the biozones and acme-zones proposed in this report, based on the La2011 astronomical solution [69] and the bio-cyclostratigraphic correlation in the Zumaia reference-section [9]; (A)—bio-astrochronological correlation and astronomically calibrated ages of key-biohorizons; (B,C)—Graphic correlations to establish the age model at Zumaia, using as tie-points (key-horizons) the 405 kyr eccentricity maxima and minima, and linearly interpolating within each precession cycle.

Table 2. Magnetostratigraphical and astronomical calibrations of Danian planktic foraminiferal key biohorizons in the Caravaca and Zumaia reference sections. Stratigraphic position (cm from the KP) of key-biohorizons, and their calibrated ages (in Ma and kyr after the KP). ?: unknown.

Key-Biohorizons	Caravaca			Zumaia		
	Height cm from KP	GTS2020 Ma	kyr after KP	Height cm from KP	GTS2020 Ma	kyr after KP
KP mass extinction horizon (Dan1 base)	0	66.001	0	0	66.001	0
LOD <i>G. acme</i> (DanAZ-1 base)	0	66.001	0	0	66.001	0
LOD <i>Pv. longiapertura</i> (Dan2 base)	3	65.996	5	6	65.994	7
LOD <i>Pv-Pg acme</i> (DanAZ-2 base)	5	65.993	8	6	65.994	7
LOD <i>Pv. eugubina</i> (Dan3a base)	22	65.982	19	23	65.983	18
LOD <i>E. simplicissima</i> (Dan3b base)	42	65.970	31	37	65.975	26
LOD <i>W-Ch acme</i> (DanAZ-3 base)	55	65.963	38	55	65.959	42
LOD <i>P. pseudobulloides</i> (Dan4a base)	107	65.933	68	100	65.933	68
LOD <i>S. triloculinoides</i> (Dan4b base)	332	65.803	198	330	65.791	210
lower/upper DanAZ-3	430	65.746	255	365	65.760	241
LOD <i>G. compressa</i> (Dan4c base)	655	65.441	560	655	65.528	473
LOD <i>E-S-P-Gl-Pr</i> dominance (DanAZ-3 top)	?	?	?	–	–	–
LOD <i>A. trinidadensis</i> (Dan4c top)	1700	63.888	2113	–	–	–

We do not currently possess precise bio-magnetostratigraphical and astronomical calibrations for the LOD of *A. trinidadensis*. At Caravaca, this key biohorizon is placed ~1700 cm above the KP [32]. According to the age model of Caravaca, the LOD of *A. trinidadensis* is calibrated ~2113 kyr after the KP (Figure 4; Table 2). We also do not possess detailed quantitative studies in the >63 µm size-fraction to accurately calibrate the HOD of the *Woodringina-Chiloguembelina* acme. Preliminary quantitative studies at some localities, such as Sidi Ziane (Algeria) and IODP Site M0077 (Chicxulub impact structure), suggest that the abundance of *Woodringina* and *Chiloguembelina* markedly decreases between the LODs of *Gl. compressa* and *A. trinidadensis*. Above this biohorizon, other genera, such as *Eoglobigerina*, *Subbotina*, *Parasubbotina*, *Globanomalina*, and *Praemurica*, clearly become dominant. However, this biohorizon remains vague, at least given our current state of knowledge. The abundance of these other genera increases between the LODs of *S. triloculinoides* and *Gl. compressa*, becoming codominant, or even locally or occasionally more abundant than *Woodringina-Chiloguembelina* (Figure 3). In the Caravaca reference section, this quantitative change, called the “lower/upper W-Ch acme” in Table 2, occurs 430 cm above the KP, i.e., 255 kyr after the KP according to our bio-magnetostratigraphical calibrations (Figure 4). In the Zumaia reference-section, it occurs 365 cm above the KP, i.e., 241 kyr after the KP according to our astronomical calibrations (Figure 5).

6. Lower Danian Planktic Foraminiferal Qualitative Zonation

6.1. *Guembelitra cretacea* Zone (Biozone Dan1)

Full name: *Abathomphalus mayaroensis*–*Parvularugoglobigerina longiapertura* Partial-Range Interval Zone.

Author: Smit [4], emended here.

Definition: Stratigraphic interval between the HOD of *Abathomphalus mayaroensis* and the LOD of *Parvularugoglobigerina longiapertura*.

Magnetostratigraphical calibration: 0–5 kyr after the KP (66.001–65.996 Ma).

Astrostratigraphical calibration: 0–7 kyr after the KP (66.001–65.994 Ma).

Estimated age (average): 66.001–65.995 Ma (6 kyr duration).

Remarks: Biozone Dan1 (or the *Guembelitra cretacea* Zone) represents the same biostratigraphic interval as the *Mh. holmdelensis* Subzone of Arenillas et al. [24]. The latter used *Mh. holmdelensis* to name this sub-biozone, since there seemed to be strong evidence that it was a survivor of the KP mass extinction event [6,72,77,78] and the ancestor of Danian taxa, such as *Globanomalina*, *Eoglobigerina*, and/or *Praemurica* [5,29,77,79] or *Parvularugoglobigerina* [36]. However, both phylogenetic hypotheses, and even the survival of *Muricohedbergella* from the KP extinction event, have subsequently been questioned [38,39,45]. Biozone Dan1 is also equivalent to Biozone P0 of Smit et al. [4,18], but they differ in their upper boundary: the LOD of *Pv. longiapertura* for Dan1 and the LOD of *Globigerina? minutula* (probably *Ps. antecessor* in this paper) for P0. It could be equivalent to Biozone M18 (the *Rugoglobigerina hexacamerata* Zone) of Blow [15], which was defined as the interval between the HOD of *Abathomphalus mayaroensis* (=KP mass extinction horizon) and the LOD of *Pv. longiapertura*. It is not strictly equivalent to Biozone P0 discussed by Wade et al. [2] and Keller et al. [23], because the former considered *Pv. longiapertura* to be a junior synonym of *Pv. eugubina*, and the latter regarded their LODs as synchronous. However, both biozones represent the same biostratigraphic interval as Dan1.

Characteristic assemblages: Except for the incoming Danian species of *Chiloguembelitra* and *Pseudocaucasina* in its upper part (Figure 2), this biozone is characterized almost exclusively by *Guembelitra* species (Figure 3). Except at Moncada (Cuba) [46], it is also characterized worldwide by abundant reworked specimens of Cretaceous species [4,33,41,79–83].

6.2. *Parvularugoglobigerina longiapertura* Zone (Biozone Dan2)

Full name: *Parvularugoglobigerina longiapertura*–*Parvularugoglobigerina eugubina* Lowest Occurrence Interval Zone.

Author: Blow [15], amended here.

Definition: Stratigraphic interval between the LOD of *Parvularugoglobigerina longiapertura* and the LOD of *Parvularugoglobigerina eugubina*.

Magnetostratigraphical calibration: 5–19 kyr after the KP (65.996–65.982 Ma).

Astrostratigraphical calibration: 7–18 kyr after the KP (65.994–65.983 Ma).

Estimated age (average): 65.995–65.983 Ma (12 kyr duration).

Remarks: Biozone Dan2 (or the *Pv. longiapertura* Zone) represents the same biostratigraphic interval as the *Parvularugoglobigerina longiapertura* Subzone identified by Arenillas et al. [24] (Figure 2), which has been elevated to biozone rank in this paper. It probably spans the lower part of Biozones P α identified by Wade et al. [2], P1a identified by Smit and Romein [18], and P1a identified by Keller et al. [23], because these authors considered *Pv. longiapertura* to be a junior synonym of *Pv. eugubina*, or their LODs to be synchronous. *Pv. longiapertura* has also been used as an index species by several authors [15,24,53,77], because it has a very distinct morphology, with a high slit-like aperture, unlike *Pv. eugubina* s.s. [36]. Biozone Dan2 is not strictly equivalent to Biozone P α (the *Globorotalia (Turborotalia) longiapertura* Zone), discussed by Blow [15], because the top of the latter was defined as the LOD of *Parasubbotina pseudobulloides*. It could be equivalent to the *Globigerina fringa* Zone, discussed by Herm et al. [84], which these authors placed below the *Globigerina eugubina* Zone. However, it seems more plausible that the *Globigerina fringa* Zone is equivalent to Sub-biozone Dan3b (the *E. simplicissima* Subzone), because the LOD of *Eoglobigerina fringa* is close to the LOD of *E. simplicissima*.

Characteristic assemblages: This biozone is characterized by the predominance of parvularugoglobigerinids (Figure 3), especially featuring species of *Parvularugoglobigerina* with flattened tests and a high-arched aperture, such as *Pv. longiapertura* (var. *euskalherriensis*), *Pv. umbrica*, and *Pg. perexigua*. Species of *Palaeoglobigerina* are also common.

6.3. *Parvularugoglobigerina eugubina* Zone (Biozone Dan3)

Full name: *Parvularugoglobigerina eugubina*–*Parasubbotina pseudobulloides* Lowest-Occurrence Interval Zone.

Author: Luterbacher and Premoli Silva [3], amended Bolli [12] and Premoli Silva and Bolli [85].

Definition: Stratigraphic interval between the LOD of *Parvularugoglobigerina eugubina* and the LOD of *Parasubbotina pseudobulloides*.

Magnetostratigraphical calibration: 19–68 kyr after the KP (65.982–65.933 Ma).

Astrostratigraphical calibration: 18–68 kyr after the KP (65.983–65.933 Ma).

Estimated age (average): 65.983–65.933 Ma (50 kyr duration).

Remarks: Biozone Dan3 (the *Parvularugoglobigerina eugubina* Zone) was originally defined by Luterbacher and Premoli Silva [3] as the total range interval of the earliest Danian assemblages composed of parvularugoglobigerinids, specifically of *Pv. eugubina*. However, the base of the subsequent biozone, i.e., the *P. pseudobulloides* Zone, was later defined as the LOD of *P. pseudobulloides* and not as the HOD of *Pv. eugubina* [12,17,85], assuming that both key-biohorizons were synchronous. For this reason, Molina et al. [34,86] considered that the original definition of the *Pv. eugubina* Zone had actually been emended, placing its top at the LOD of *P. pseudobulloides* because this species features a greater taxonomic consensus. The original definition was nonetheless maintained by Wade et al. [2] for their equivalent Biozone P α , and by Keller et al. [23] for their equivalent Biozone P1a (Figure 2).

Characteristic assemblages: See the characteristic assemblages in each sub-biozone of Dan3.

6.3.1. *Parvularugoglobigerina sabina* Subzone (Sub-Biozone Dan3a)

Full name: *Parvularugoglobigerina eugubina*–*Eoglobigerina simplicissima* Lowest-occurrence Interval Subzone.

Author: Arenillas et al. [24].

Definition: Stratigraphic interval between the LOD of *Parvularugoglobigerina eugubina* and the LOD of *Eoglobigerina simplicissima*.

Magnetostratigraphical calibration: 19–31 kyr after the KP (65.982–65.970 Ma).

Astrostratigraphical calibration: 18–26 kyr after the KP (65.983–65.975 Ma).

Estimated age (average): 65.983–65.973 Ma (10 kyr duration).

Remarks: Sub-biozone Dan3a (the *Pv. sabina* Subzone) is the same as the *Pv. sabina* Subzone identified by Arenillas et al. [24] (Figure 2). *Pv. sabina* has commonly been considered a junior synonym of *Pv. eugubina* [17,28,29,85]. However, Arenillas et al. distinguished them according to the original meaning given to both species [3,36].

Characteristic assemblages: This is an interval still dominated by smooth-walled parvularugoglobigerinids (Figure 3). It is characterized by *Parvularugoglobigerina* species with globular chambers and a low-arch aperture, such as *Pv. eugubina* and *Pv. sabina*.

6.3.2. *Eoglobigerina simplicissima* Subzone (Sub-Biozone Dan3b)

Full name: *Eoglobigerina simplicissima*–*Parasubbotina pseudobulloides* Lowest-Occurrence Interval Subzone.

Author: Arenillas et al. [24].

Definition: Stratigraphic interval between the LOD of *Eoglobigerina simplicissima* and the LOD of *Parasubbotina pseudobulloides*.

Magnetostratigraphical calibration: 31–68 kyr after the KP (65.970–65.933 Ma).

Astrostratigraphical calibration: 26–68 kyr after the KP (65.975–65.933 Ma).

Estimated age (average): 65.973–65.933 Ma (40 kyr duration).

Remarks: Subbiozone Dan3b (the *E. simplicissima* Subzone) is the same as the *E. simplicissima* Subzone of Arenillas et al. [24] (Figure 2), who established it to include a very relevant key-biohorizon among planktic foraminiferal zonations: the LOD of Danian species with a cancellate/pitted wall texture (*Eoglobigerina* and *Globanomalina*). The LOD of *Eoglobigerina* spp. was already utilized by Smit and Romein [18] to define their Biozone P1b (the *Eoglobigerina taurica* Zone). The *Eoglobigerina eobulloides* Subzone of Luciani [87] is probably also equivalent to Subbiozone Dan3b. Although *E. simplicissima* has been considered a junior synonym of *E. eobulloides* [29], Arenillas et al. used it as an index species because it features a more distinctive and stable morphology than *E. eobulloides* [24].

Characteristic assemblages: This sub-biozone is characterized by a progressive increase in the relative abundance of *Woodringina* and *Chiloguembelina*, which become predominant towards the upper part of the sub-biozone (Figure 3). The LODs of *Eoglobigerina*, *Globanomalina*, *Trochoguembelina*, *Parasubbotina*, and *Praemurica* are recorded in this sub-biozone, the first three almost simultaneously in its basal part (Figure 2).

6.4. *Parasubbotina pseudobulloides* Zone (Biozone Dan4)

Full name: *Parasubbotina pseudobulloides*–*Acarinina trinidadensis* Lowest-Occurrence Interval Zone.

Author: Leonov and Alimarina [11], amended by Molina et al. [34].

Definition: Stratigraphic interval between the LOD of *Parasubbotina pseudobulloides* and the LOD of *Acarinina trinidadensis*.

Magnetostratigraphical calibration: 68–2113 kyr after the KP (65.933–63.888 Ma).

Astrostratigraphical calibration: 68–? kyr after the KP (65.933–? Ma).

Estimated age (average): 65.933 Ma–63.888 Ma (2045 kyr duration).

Remarks: Biozone Dan4 (the *P. pseudobulloides* Zone) was introduced by Leonov and Alimarina [11] as the *Globigerina pseudobulloides*–*Globigerina daubjergensis* Zone. Its name was later shortened to the *Globigerina pseudobulloides* Zone [12]. *P. pseudobulloides* is an index-species used in most planktic foraminiferal zonations of the lower Danian [2,17,18,23–25]. Biozone Dan4 is approximately equivalent to Biozone P1c, discussed by Smit et al. [4,18] and to that discussed by Keller et al. [21,23] (Figure 2). It is also equivalent to Biozone P1, identified by Berggren [2,13], although they span different biostratigraphic intervals because the lower and upper boundaries of P1 were defined as the HOD of *Pv. eugubina* and the LOD of *A. uncinata* respectively.

Characteristic assemblages: See the characteristic assemblages in each sub-biozone of Dan4.

6.4.1. *Praemurica taurica* Subzone (Sub-Biozone Dan4a)

Full name: *Parasubbotina pseudobulloides*–*Subbotina trilocolinoides* Lowest-Occurrence Interval Subzone.

Author: Arenillas et al. [24], renamed here.

Definition: Stratigraphic interval between the LOD of *Parasubbotina pseudobulloides* and the LOD of *Subbotina trilocolinoides*.

Magnetostratigraphical calibration: 68–198 kyr after the KP (65.933–65.803 Ma).

Astrochronological calibration: 68–210 kyr after the KP (65.933–65.791 Ma).

Estimated age (average): 65.933–65.797 Ma (136 kyr duration).

Remarks: Subbiozone Dan4a (the *Pr. taurica* Subzone) is the same as the *Eoglobigerina trivialis* Subzone of Arenillas et al. [24], except for the name (Figure 2). Since *E. trivialis* has been used in different taxonomic senses [15,29,35], we have decided to rename it using *Pr. taurica*, which features a greater taxonomic consensus. *Pr. taurica* was first used as an index species by Morozova [88,89] to define the base of the *Globigerina* (*Eoglobigerina*) *taurica* Zone (Biozone Dan₁I). Subbiozone Dan4a should not be confused with Subbiozone P1b (the *Eoglobigerina taurica* Subzone), discussed by Smit [4,18], because the latter seems equivalent rather to Subbiozone Dan3b (the *E. simplicissima* Subzone).

Characteristic assemblages: In this sub-biozone, *Woodringina* and *Chiloguembelina* remain the predominant taxa (Figure 3). *Chiloguembelitra* blooms have been identified locally in this sub-biozone [8,9,39]; these have usually been confused with *Guembelitra* blooms [73,76]. The LOD of *Globoconusa* is recorded in this sub-biozone (Figure 2).

6.4.2. *Subbotina triloculinoides* Subzone (Subbiozone Dan4b)

Full name: *Subbotina triloculinoides*–*Globanomalina compressa* Lowest-Occurrence Interval Subzone.

Author: Berggren [13], amended by Arenillas et al. [24].

Definition: Stratigraphic interval between the LOD of *Subbotina triloculinoides* and the LOD of *Globanomalina compressa*.

Magnetostratigraphical calibration: 198–560 kyr after the KP (65.803–65.441 Ma).

Astrochronological calibration: 210–473 kyr after the KP (65.791–65.528 Ma).

Estimated age (average): 65.797–65.485 Ma (312 kyr duration).

Remarks: Subbiozone Dan4b (the *S. triloculinoides* Subzone) is the same as the *S. triloculinoides* Subzone discussed by Arenillas et al. [24]. Berggren [13] was the first to use the LOD of *S. triloculinoides* as a key-biohorizon in order to define the base of Subbiozone P1b (or the *Globigerina triloculinoides* Subzone). The *Globigerina microcellulosa* Zone (Biozone Dan₁II) of Morozova [88,89] could be equivalent, although the LOD of *Eoglobigerina microcellulosa* is placed at a stratigraphical position lower than the LOD of *S. triloculinoides*. Subbiozone P1b, discussed by Berggren [13] and Wade et al. [2], should not be confused with Biozones P1b (the *Eoglobigerina taurica* Subzone) of Smit [4] and P1b (unnamed) of Keller et al. [23], which comprise different biostratigraphic intervals (Figure 2).

Characteristic assemblages: The LOD of *Subbotina* is recorded in this sub-biozone (Figure 2). Although *Woodringina* and *Chiloguembelina* remain the dominant taxa, *Eoglobigerina*, *Globanomalina*, *Parasubbotina*, *Praemurica*, and *Subbotina* progressively increase their relative abundance. The relative abundance of these taxa locally or sporadically exceeds that of *Woodringina* and *Chiloguembelina* (Figure 3).

6.4.3. *Globanomalina compressa* Subzone (Sub-Biozone Dan4c)

Full name: *Globanomalina compressa*–*Acarinina trinidadensis* Lowest-Occurrence Interval Subzone.

Author: Berggren [13], amended by Arenillas and Molina [32].

Definition: Stratigraphic interval between the LOD of *Globanomalina compressa* and the LOD of *Acarinina trinidadensis*.

Magnetostratigraphical calibration: 560–2113 kyr after the KP (65.441–63.888 Ma).

Astrochronological calibration: 473–? kyr after the KP (65.528–? Ma).

Estimated age (average): 65.485–63.888 Ma (1597 kyr duration).

Remarks: Subbiozone Dan4c (the *Gl. compressa* Subzone) spans the same biostratigraphic interval as the *Gl. compressa* Zone identified by Molina et al. [32,34]. Berggren [13] was the first to use the LOD of *Gl. compressa* as a key biohorizon in order to define the base of Subbiozone P1c [2,19,22,26]. This sub-biozone should not be confused with Biozone P1c (the *Globigerina pseudobulloides* Zone) discussed by Smit [4] and P1c (the *Subbotina pseudobulloides* Zone) discussed by Keller et al. [23] since these are roughly equivalent to the entire Biozone Dan4 (the *P. pseudobulloides* Zone) (Figure 2).

Characteristic assemblages: This sub-biozone is characterized by the predominance of *Eoglobigerina*, *Globanomalina*, *Parasubbotina*, *Praemurica*, and *Subbotina*, although *Woodringina* and *Chiloguembelina* are still common, being sporadically dominant especially in the lower part of the sub-biozone (Figure 3).

7. Lower Danian Planktic Foraminiferal Acme-Zonation

7.1. *Guembelitra* Abundance Zone (Acme-Zone DanAZ1)

Definition: Stratigraphic interval between the LOD of *Guembelitra* dominance and the LOD of *Parvularugoglobigerina* dominance.

Magnetostratigraphical calibration: 0–8 kyr after the KP (66.001–65.993 Ma).

Astrostratigraphical calibration: 0–7 kyr after the KP (66.001–65.994 Ma).

Estimated age (average): 66.001–65.993 Ma (8 kyr duration).

Remarks: Acme zone DanAZ1 spans from the KP to the middle part of Biozone Dan2 and is characterized by the apogee of *Guembelitra*. This *Guembelitra* acme should not be confused with other triserial guembelitriid blooms identified both in the Maastrichtian and Danian, the latter characterized by *Chiloguembelitra* and not by *Guembelitra*. The *Guembelitra* acme after the KP mass extinction has also been recognized in quantitative studies carried out in the >38 µm size fraction [90,91]. The explosive increase in the relative abundance of *Guembelitra* may only be apparent, as it was the only genus that survived the KP mass extinction [38,46]. In terms of absolute abundance, its increase seems not to have been so significant [40,41]. This biostratigraphic interval is also characterized by a bloom of aberrant guembelitriids [8,39], which have sometimes been assigned to the species *Guembelitra irregularis* [92]. In the lowermost Danian of most sections, the *Guembelitra* acme of DanAZ1 is also masked by the high abundance of reworked specimens of other Cretaceous species [4,40–42,80–83].

7.2. *Parvularugoglobigerina*-*Palaeoglobigerina* Abundance Zone (Acme Zone DanAZ2)

Definition: Stratigraphic interval between the LOD of *Parvularugoglobigerina* and *Palaeoglobigerina* dominance and the LOD of *Woodringina*-*Chiloguembelina* dominance.

Magnetostratigraphical calibration: 8–38 kyr after the KP (65.993–65.963 Ma).

Astrostratigraphical calibration: 7–42 kyr after the KP (65.994–65.959 Ma).

Estimated age (average): 65.993–65.961 Ma (32 kyr duration)

Remarks: Acme zone DanAZ2 spans from the middle part of Biozone Dan2 to the middle part of Subbiozone Dan3b and is characterized by the apogee of parvularugoglobigerinids, i.e., of tiny (usually <150 µm), smooth-walled, trochospiral species belonging to the genera *Parvularugoglobigerina* and *Palaeoglobigerina*. They should not be confused with more modern and larger (usually >150 µm) trochospiral species with pore-mounded, rugose walls belonging to the genus *Trochoguembelitra*, whose first appearance roughly coincides with those of *Eoglobigerina* and *Globanomalina*.

7.3. *Woodringina*-*Chiloguembelina* Abundance Zone (Acme Zone DanAZ3)

Definition: Stratigraphic interval between the LOD of *Woodringina*-*Chiloguembelina* dominance and the LOD of *Eoglobigerina*-*Subbotina*-*Parasubbotina*-*Globanomalina*-*Praemurica* dominance.

Magnetostratigraphical calibration: 38–? kyr after the KP (65.963–? Ma).

Astrostratigraphical calibration: 42–? kyr after the KP (65.959–? Ma).

Estimated age (average): 65.961–? Ma (>1500 kyr duration)

Remarks: Acme-zone DanAZ3 spans from the middle part of Sub-biozone Dan3b to the lower part of Subbiozone Dan4c and is characterized by the dominance of biserial species of *Woodringina* and *Chiloguembelina*. However, two distinct intervals can be recognized (Figure 3). The first spans from the middle part of Sub-biozone Dan3b to the lower part of Subbiozone Dan4b and is characterized by the clear dominance of biserial species, except sporadically for *Chiloguembelitra blooms* (dark green shading in Figure 3). The second spans from the lower part of Subbiozone Dan4b to the lower part of Sub-biozone Dan4c and is characterized by a shared domain with the genera *Eoglobigerina*, *Subbotina*, *Parasubbotina*, *Globanomalina*, and *Praemurica* (light green shading in Figure 3). The boundary between the two intervals is not precise, but bio-magnetostratigraphical calibrations date it to approximately 255 kyr after the KP, and the astronomical calibrations to 241 kyr after the KP (with an average of 248 kyr after the KP, and an estimated age of 65.753 Ma). The latter genera become dominant approximately from the middle part of Subbiozone Dan4c, so a fourth acme stage (PFAS-4) came to be recognized above PFAS-3, i.e., above Acme zone DanAZ3, as defined here [32]. However, we do not possess enough quantitative biostratigraphic studies in sections of different regions to demonstrate its lateral traceability or biostratigraphic utility.

Supplementary Materials: The following are available online at <https://www.mdpi.com/article/10.3390/geosciences11110479/s1>. Table S1: Detailed data for the magnetostratigraphical calibration of lower Danian planktic foraminiferal key biohorizons in the Caravaca reference-section. Stratigraphic position (cm from the KP) of tie-points and key-biohorizons, and their calibrated ages (in Ma and kyr after the KP) according to GTS 2020 [54]. G. acme = *Guembelitra* acme; Pv-Pg acme = *Parvularugoglobigerina-Palaeoglobigerina* acme; W-Ch acme = *Woodringina-Chiloguembelina* acme. Lower/upper DanAZ3: codominance of *Woodringina-Chiloguembelina* and other genera (*Eoglobigerina-Subbotina-Parasubbotina-Globanomalina-Praemurica*); E-S-P-Gl-Pr dominance: *Eoglobigerina-Subbotina-Parasubbotina-Globanomalina-Praemurica* dominance. Table S2: Detailed data for the astrostratigraphical calibration of lower Danian planktic foraminiferal key biohorizons in the Zumaia reference-section. Stratigraphic position (cm from the KP) of tie-points (405 kyr maximum and minimum, and base of precession cycles) and key biohorizons, and their calibrated ages (in Ma and kyr after the KP) according to GTS 2020 [54]. G. acme = *Guembelitra* acme; Pv-Pg acme = *Parvularugoglobigerina-Palaeoglobigerina* acme; W-Ch acme = *Woodringina-Chiloguembelina* acme; lower/upper DanAZ3: codominance of *Woodringina-Chiloguembelina* and other genera (*Eoglobigerina-Subbotina-Parasubbotina-Globanomalina-Praemurica*). E-S-P-Gl-Pr dominance: *Eoglobigerina-Subbotina-Parasubbotina-Globanomalina-Praemurica* dominance. Text S1: Main diagnostic characters of the Danian planktic foraminiferal species and genera considered in this paper.

Author Contributions: Conceptualization, I.A., V.G. and J.A.A.; methodology, I.A., V.G. and J.A.A.; formal analysis, I.A. and V.G.; investigation, I.A., V.G. and J.A.A.; resources, I.A., V.G. and J.A.A.; writing—original draft preparation, I.A. All authors have read and agreed to the published version of the manuscript.

Funding: This research is part of the grants PGC2018-093890-B-I00 funded by MCIN/AEI/10.13039/501100011033 and ERDF A way of making Europe, and DGA group E33_20R funded by the Aragonese Government and ERDF A way of making Europe. V. Gilabert acknowledges the grant BES-2016-077800 funded by MCIN/AEI/10.13039/501100011033 and ESF Investing in your future.

Data Availability Statement: Not applicable.

Acknowledgments: We would like to thank the valuable comments of reviewers, which have contributed substantially to the improvement of this work. We thank R. Glasgow for improving the English text. We would also like to thank the Servicio General de Apoyo a la Investigación-SAI of the Universidad de Zaragoza for the SEM photographs.

Conflicts of Interest: The authors declare no conflict of interest.

Appendix A

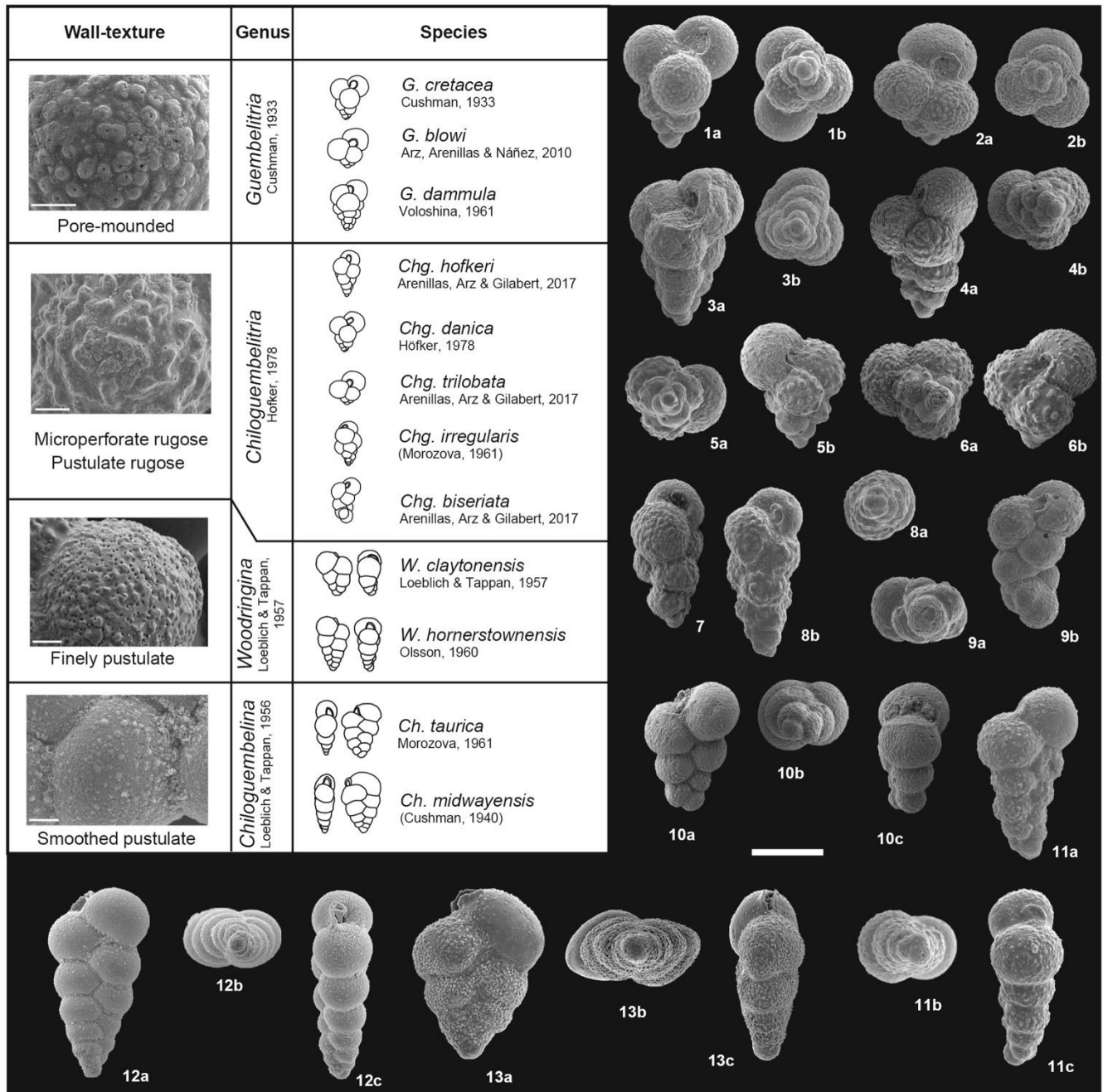


Figure A1. Species of *Guembelitra*, *Chiloguembelitra*, *Woodringina*, and *Chiloguembelina*. For taxonomic comparisons, the Maastrichtian species *Guembelitra dammula* is also included. 1. *Guembelitra cretacea*; 2. *G. blowi*; 3. *G. dammula*; 4. *Chiloguembelitra danica*; 5–6. *Chg. irregularis*; 7. *Chg. hofkeri*; 8. *Chg. trilobata*; 9. *Chg. biseriata*; 10. *Woodringina claytonensis*; 11. *W. hornerstownensis*; 12. *Chiloguembelina taurica*; 13. *Ch. midwayensis*. See main diagnostic characters of these species and genera in Supplementary Text S1. All specimens are from El Kef, except those from Ain Settara (10, 11), DSDP Site 305 (12), and Ben Gurion (13). Scale bar = 100 µm.

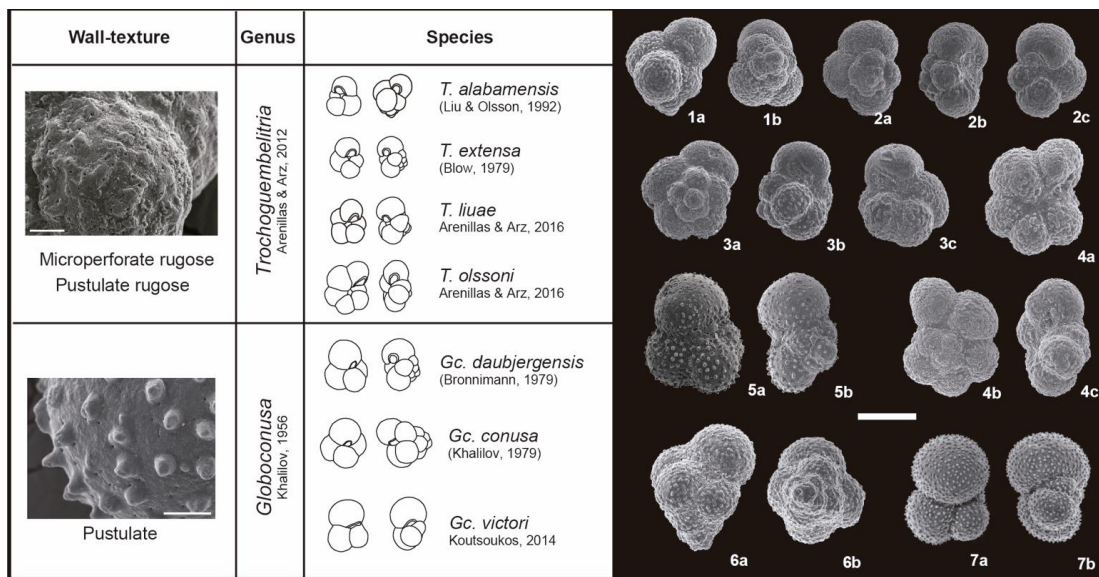


Figure A2. Species of *Trochoguembelitra* and *Globoconusa*. 1. *Trochoguembelitra alabamensis*; 2. *T. extensa*; 3. *T. liuae*; 4. *T. olssoni*; 5. *Globoconusa daubjergensis*; 6. *Gc. conusa*; 7. *Gc. victori*. See main diagnostic characters of these species and genera in Supplementary Text S1. Specimens are from El Kef (1–4), Bajada del Jagüel (5), Ben Gurion (6), and Campos Basin, offshore Brazil (7; specimen reported by Koutsoukos [5]). Scale bar = 100 µm.

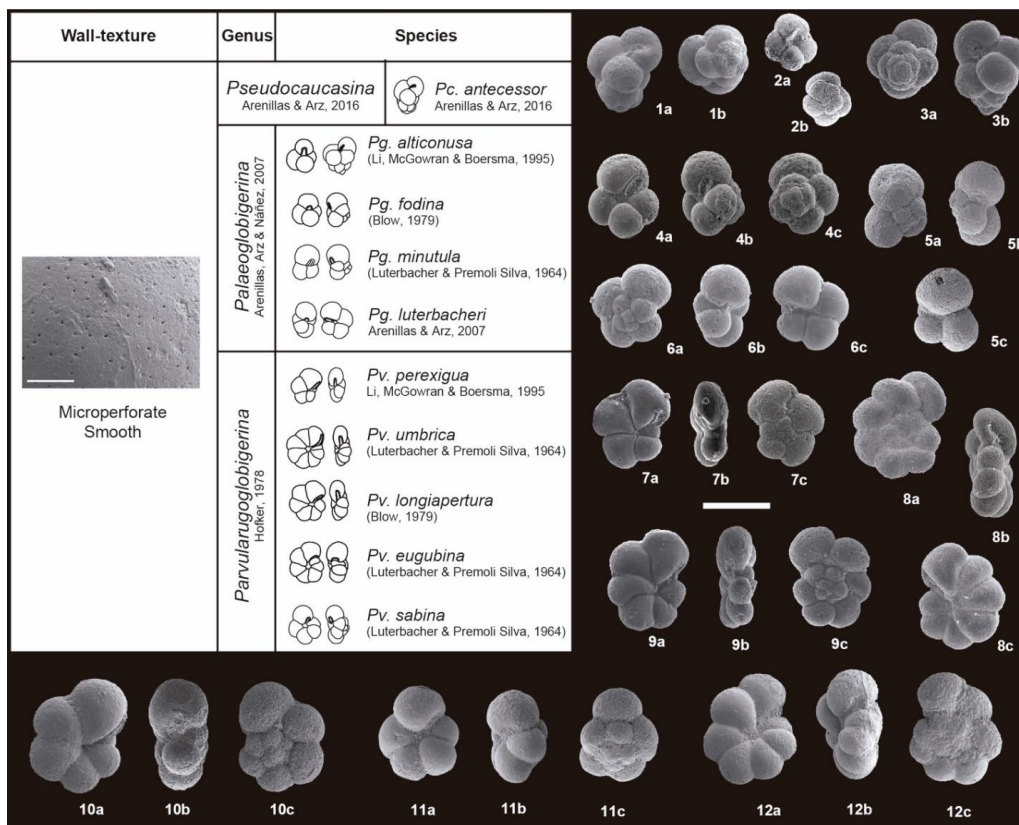


Figure A3. Species of *Pseudocaucasina*, *Palaeoglobigerina*, and *Parvularugoglobigerina*. 1. *Pseudocaucasina antecessor*; 2. *Ps. antecessor*, juvenile specimen; 3. *Palaeoglobigerina alticonusa*; 4. *Palaeoglobigerina fodina*; 5. *Pg. minutula*; 6. *Pg. luterbacheri*; 7. *Parvularugoglobigerina perexigua*; 8. *Pv. umbrica*; 9. *Pv. longiapertura* (var. *euskalherriensis*); 10. *Pv. longiapertura* (var. *longiapertura*); 11. *Pv. sabina*; 12. *Pv. eugubina*. See main diagnostic characters of these species and genera in Supplementary Text S1. Specimens are from El Kef (1–8,11,12), and Ain Settara (9,10); juvenile specimen of *Pseudocaucasina antecessor* (2) reported by Brinkhuis and Zachariasse [93]. Scale bar = 100 µm.

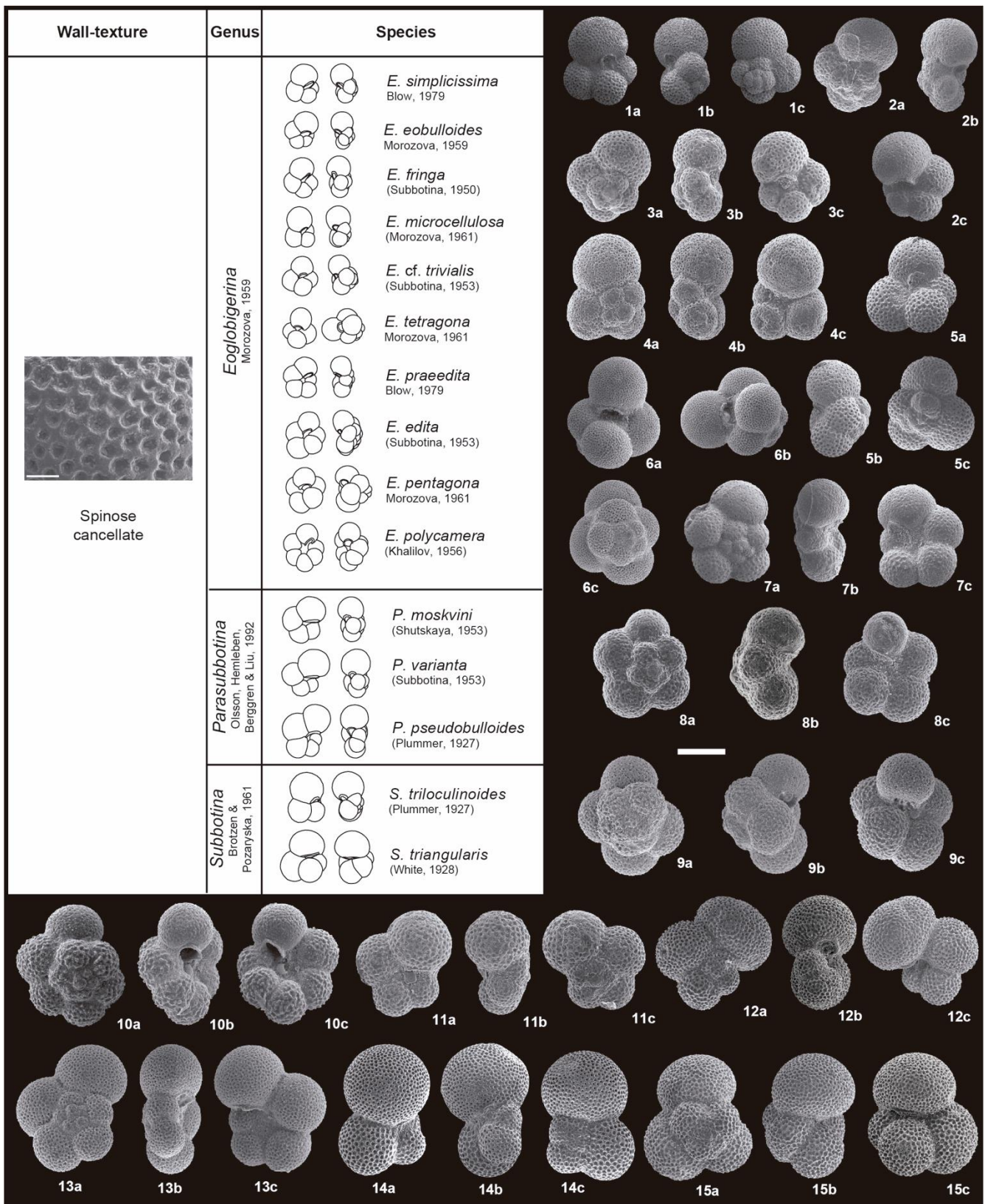


Figure A4. Early Danian species of *Eoglobigerina*, *Parasubbotina*, and *Subbotina*. 1. *Eoglobigerina simplicissima*; 2. *E. eobulloides*; 3. *E. fringa*; 4. *E. microcellulosa*; 5. *E. cf. trivialis*; 6. *E. tetragona*; 7. *E. praedita*; 8. *E. edita*; 9. *E. pentagona*; 10. *E. polycamera*; 11. *Parasubbotina moskvini*; 12. *P. varianta*; 13. *P. pseudobulloides*; 14. *Subbotina triloculinoides*; 15. *S. triangularis*. See main diagnostic characters of these species and genera in Supplementary Text S1. Specimens are from El Kef (1–4,7), Ben Gurion (5,8,11,12,15), Gebel Aweina (14), and DSDP Site 305 (6,9,10,13). Scale bar = 100 μ m.

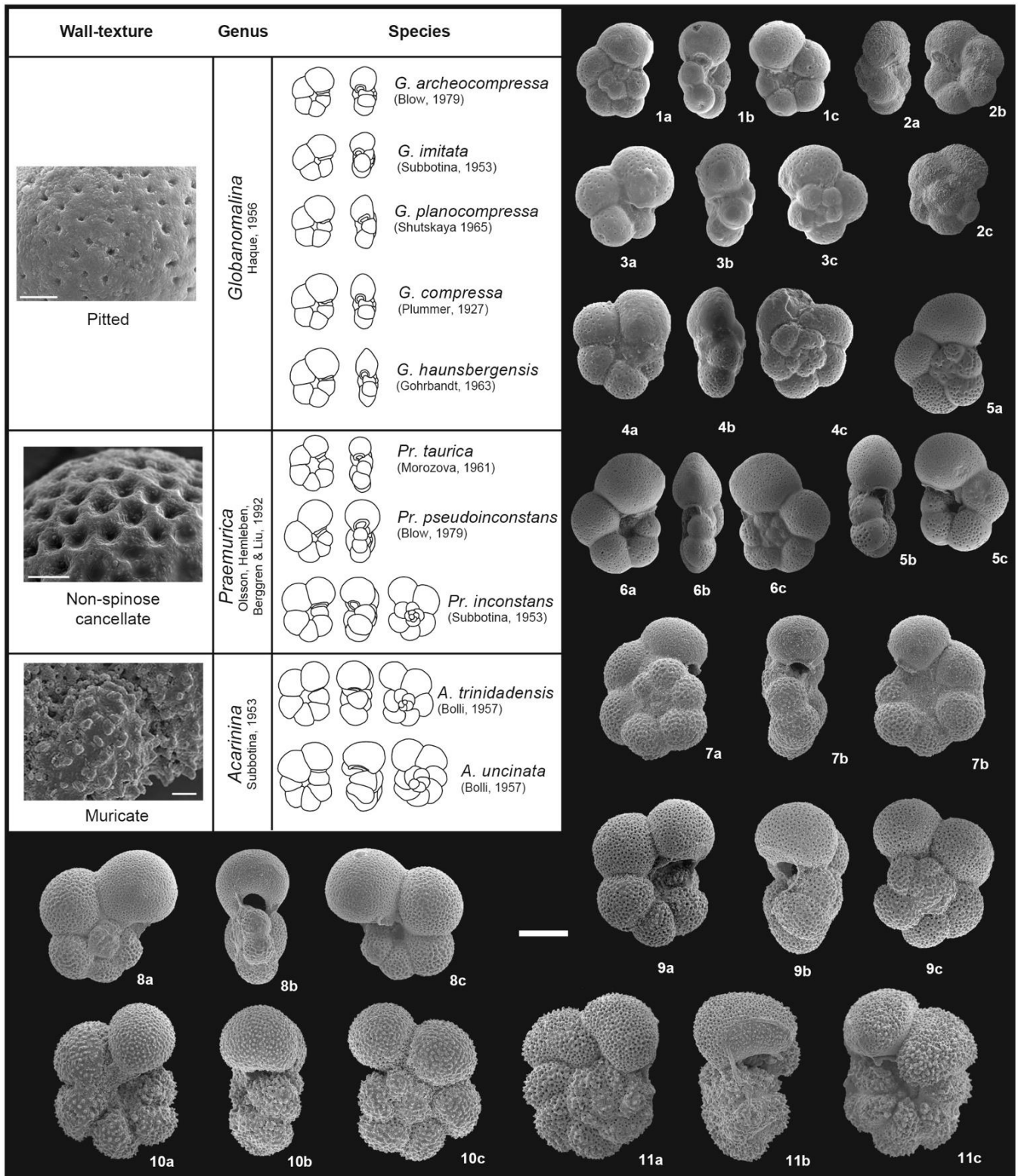


Figure A5. Early Danian species of *Globanomalina* and *Praemurica*. For taxonomic comparisons, the middle Danian species *Globanomalina haunsbergensis*, *Acarinina trinidadensis* and *A. uncinata* are also included. 1-2. *Globanomalina archeocompressa*; 3. *Gl. imitata*; 4. *Gl. planocompressa*; 5. *Gl. compressa*; 6. *Gl. haunsbergensis*; 7. *Praemurica taurica*; 8. *Pr. pseudoinconstans*; 9. *Pr. inconstans*; 10. *Acarinina trinidadensis*; 11. *A. uncinata*. See main diagnostic characters of these species and genera in Supplementary Text S1. Specimens are from El Kef (1–4), Sidi Nasseur (5,6), and DSDP Site 305 (7–11). Scale bar = 100 µm.

References

1. Bolli, H.M. The genera *Globigerina* and *Globorotalia* in the Paleocene-lower Eocene Lizard Springs formation of Trinidad, B.W.I. *US Nat. Mus. Bull.* **1957**, *215*, 97–124.
2. Wade, B.R.; Pearson, P.N.; Berggren, W.A.; Pälike, H. Review and revision of Cenozoic tropical planktonic foraminiferal biostratigraphy and calibration to the geomagnetic polarity and astronomical time scale. *Earth-Sci. Rev.* **2011**, *104*, 111–142. [[CrossRef](#)]
3. Luterbacher, H.P.; Premoli Silva, I. Biostratigrafia del limite Cretaceo-Terziario nell'Apennino Centrale. *Riv. Ital. Paleontol. Stratigr.* **1964**, *70*, 67–128.
4. Smit, J. Extinction and evolution of planktonic foraminifera after a major impact at the Cretaceous/Tertiary boundary. *Geol. Soc. Am. Spec. Pap.* **1982**, *190*, 329–352. [[CrossRef](#)]
5. Koutsoukos, E.A. Phenotypic plasticity, speciations, and phylogeny in Early Danian planktic foraminifera. *J. Foraminifer. Res.* **2014**, *44*, 109–142. [[CrossRef](#)]
6. Lowery, C.M.; Bralower, T.J.; Owens, J.D.; Rodríguez-Tovar, F.J.; Jones, H.; Smit, J.; Whalen, M.T.; Claeys, P.; Farley, K.; Gulick, S.P.S.; et al. Rapid recovery of life at ground zero of the end-Cretaceous mass extinction. *Nature* **2018**, *558*, 288–291. [[CrossRef](#)]
7. Krahl, G.; Bom, M.H.H.; Kochhann, K.G.D.; Souza, L.V.; Savian, J.F.; Fauth, G. Environmental changes occurred during the Early Danian at the Rio Grande Rise, South Atlantic Ocean. *Glob. Planet. Chang.* **2020**, *191*, 103197. [[CrossRef](#)]
8. Gilabert, V.; Arenillas, I.; Arz, J.A.; Batenburg, S.J.; Robinson, S.A. Multiproxy analysis of paleoenvironmental, paleoclimatic and paleoceanographic changes during the early Danian in the Caravaca section (Spain). *Palaeogeogr. Palaeoclimatol. Palaeoecol.* **2021**, *576*, 110513. [[CrossRef](#)]
9. Gilabert, V.; Batenburg, S.J.; Arenillas, I.; Arz, J.A. Contribution of orbital forcing and Deccan volcanism to global climatic and biotic changes across the KPB at Zumaia, Spain. *Geology* **2021**, *49*, in press. [[CrossRef](#)]
10. Subbotina, N.N. Iskopaemye Foraminifery SSSR Globigerinidy, Khantkeninidy i Globorotaliidy [Fossil Foraminifera of the USSR. Globigerinidae, Hantkeninidae and Globorotaliidae]. *Trudy Vses. Neft. Nauchno-Issled. Geol.-Razved. Inst. (VNIGRI)* **1953**, *76*, 1–296.
11. Leonov, G.P.; Alimarina, V.P. Stratigraphy and foraminifera of Cretaceous-Paleogene “transition” beds of the central part of the North Caucasus. *Mosc. Univ. Geol. Fac. Sb. Tr.* **1961**, 29–60.
12. Bolli, H.M. Zonación de sedimentos marinos del Cretáceo hasta el Plioceno, basada en foraminíferos planctónicos. *Bol. inf. Asoc. Venez. Geol. Min. Petrol.* **1966**, *9*, 1–34.
13. Berggren, W.A. Rates of evolution in some Cenozoic planktonic foraminifera. *Micropaleontology* **1969**, *15*, 351–365. [[CrossRef](#)]
14. Berggren, W.A. Multiple phylogenetic zonations of the Cenozoic based on planktonic foraminifera. In Proceedings of the II Planktonic Conference, Roma, Italy, 29 September–7 October 1970; Farinacci, A., Ed.; Edizioni Tecnoscienza: Roma, Italy, 1971; pp. 41–56.
15. Blow, W.H. The Cainozoic Globigerinida: A study of the morphology, taxonomy, evolutionary relationship and the stratigraphical distribution of some Globigerinidae (mainly Globigerinacea). *E. J. Brill Leiden* **1979**, *3*, 1413.
16. Stainforth, R.M.; Lamb, J.L.; Luterbacher, H.P.; Beardand, J.H.; Jeffords, R.M. *Cenozoic Planktonic Foraminiferal Zonation and Characteristics of Index Form*; University of Kansas Library: Lawrence, KS, USA, 1975; 425p.
17. Toumarkine, M.; Luterbacher, H.P. Paleocene and Eocene planktic foraminifera. In *Plankton Stratigraphy*; Bolli, H.M., Saunders, J.B., Perch-Nielsen, K., Eds.; Cambridge University Press: Cambridge, UK, 1985; pp. 87–154.
18. Smit, J.; Romein, A.J.T. A sequence of events across the Cretaceous-Tertiary boundary. *Earth Planet. Sci. Lett.* **1985**, *74*, 155–170. [[CrossRef](#)]
19. Berggren, W.A.; Miller, K.G. Paleogene tropical planktonic foraminiferal biostratigraphy and magnetobiochronology. *Micropaleontology* **1988**, *34*, 362–380. [[CrossRef](#)]
20. Keller, G. Extinction, survivorship and evolution of planktic foraminifera across the Cretaceous/Tertiary boundary at El Kef, Tunisia. *Mar. Micropaleontol.* **1988**, *13*, 239–263. [[CrossRef](#)]
21. Keller, G. The Cretaceous/Tertiary boundary transitions in the Antarctic Ocean and its global implications. *Mar. Micropaleontol.* **1993**, *21*, 1–45. [[CrossRef](#)]
22. Berggren, W.A.; Kent, D.V.; Swisher, C.C., III; Aubry, M.P. A revised Paleogene Geochronology and Chronostratigraphy. In *Geochronology, Time Scales and Global Stratigraphic Correlation*; Berggren, W.A., Kent, D.V., Aubry, M.P., Hardenbol, J., Eds.; SEPM Sp. Pub.: Broken Arrow, OK, USA, 1995; Volume 54, pp. 129–213. [[CrossRef](#)]
23. Keller, G.; Li, L.; MacLeod, N. The Cretaceous/Tertiary boundary stratotype sections at El Kef, Tunisia: How catastrophic was the mass extinction? *Palaeogeogr. Palaeoclimatol. Palaeoecol.* **1995**, *119*, 221–254. [[CrossRef](#)]
24. Arenillas, I.; Arz, J.A.; Molina, E. A new high-resolution planktic foraminiferal zonation and subzonation for the lower Danian. *Lethaia* **2004**, *37*, 79–95. [[CrossRef](#)]
25. Rasmussen, J.A.; Heinberg, C.; Håkansson, E. Planktonic foraminifera, biostratigraphy and the diachronous nature of the lowermost Danian Cerithium Limestone at Stevns Klint, Denmark. *Bull. Geol. Soc. Den.* **2005**, *52*, 113–131. [[CrossRef](#)]
26. Berggren, W.A.; Pearson, P.N. A revised tropical to subtropical Paleogene planktonic foraminiferal zonation. *J. Foraminifer. Res.* **2005**, *35*, 279–298. [[CrossRef](#)]

27. Berggren, W.A. Atlas of Paleogene Planktonic Foraminifera. Some species of the genera *Subbotina*, *Planorotalites*, *Morozovella*, *Acarinina* and *Truncorotaloides*. In *Oceanic Micropaleontology*; Ramsay, A.T.S., Ed.; Academic Press: London, UK, 1977; Volume 1, pp. 250–299.
28. Berggren, W.A.; Norris, R.D. Biostratigraphy, phylogeny and systematics of Paleocene trochospiral planktic foraminifera. *Micropaleontology* **1997**, *43*, 1–116. [[CrossRef](#)]
29. Olsson, R.K.; Hemleben, C.; Berggren, W.A.; Huber, B.T. Atlas of Paleocene Planktonic Foraminifera. *Smithson. Contrib. Paleobiol.* **1999**, *85*, 1–252. [[CrossRef](#)]
30. Molina, E.; Alegret, L.; Arenillas, I.; Arz, J.A.; Gallala, N.; Grajales-Nishimura, M.; Murillo-Muñetón, G.; Zaghbib-Turki, D. The Global Boundary Stratotype Section and Point for the base of the Danian Stage (Paleocene, Paleogene, “Tertiary”, Cenozoic): Auxiliary sections and correlation. *Episodes* **2009**, *32*, 84–95. [[CrossRef](#)]
31. Arz, J.A.; Arenillas, I.; Molina, E.; Sepúlveda, R. La estabilidad faunística de foraminíferos planctónicos en el Maastrichtiense superior y su extinción en masa catastrófica en el límite K/T de Caravaca, España. *Rev. Geol. Chile* **2000**, *27*, 27–47. [[CrossRef](#)]
32. Arenillas, I.; Molina, E. Análisis cuantitativo de los foraminíferos planctónicos del Paleoceno de Caravaca (Cordilleras Béticas): Cronoestratigrafía, bioestratigrafía y evolución de las asociaciones. *Rev. Esp. Paleontol.* **1997**, *12*, 207–232.
33. Arenillas, I.; Arz, J.A.; Molina, E. El límite Cretácico/Terciario de Zumaya, Osinaga y Músquiz (Pirineos): Control bioestratigráfico y cuantitativo de hiatus con foraminíferos planctónicos. *Rev. Soc. Geol. Esp.* **1998**, *11*, 127–138.
34. Molina, E.; Arenillas, I.; Arz, J.A. The Cretaceous/Tertiary boundary mass extinction in planktic foraminifera at Agost (Spain). *Rev. Micropaleontol.* **1996**, *39*, 225–243. [[CrossRef](#)]
35. Metsana-Oussaid, F.; Belhai, D.; Arenillas, I.; Arz, J.A.; Gilabert, V. New sections of the Cretaceous-Paleogene transition in the southwestern Tethys (Médéa, northern Algeria): Planktic foraminiferal biostratigraphy and biochronology. *Arabian J. Geosciences* **2019**, *12*, 217. [[CrossRef](#)]
36. Arenillas, I.; Arz, J.A. *Parvularugoglobigerina eugubina* type-sample at Ceselli (Italy): Planktic foraminiferal assemblage and lowermost Danian biostratigraphic implications. *Riv. Ital. Paleontol. Stratigr.* **2000**, *106*, 379–390.
37. Molina, E.; Alegret, L.; Arenillas, I.; Arz, J.A.; Gallala, N.; Hardenbol, J.; von Salis, K.; Steurbaut, E.; Vandenberghe, N.; Zaghbib-Turki, D. The Global Stratotype Section and Point of the Danian Stage (Paleocene, Paleogene, “Tertiary”, Cenozoic) at El Kef, Tunisia: Original definition and revision. *Episodes* **2006**, *29*, 263–278. [[CrossRef](#)]
38. Arenillas, I.; Arz, J.A. Benthic origin and earliest evolution of the first planktonic foraminifera after the Cretaceous/Paleogene boundary mass extinction. *Hist. Biol.* **2017**, *29*, 17–24. [[CrossRef](#)]
39. Arenillas, I.; Arz, J.A.; Gilabert, V. Blooms of aberrant planktic foraminifera across the KPB in the Western Tethys: Causes and evolutionary implications. *Paleobiology* **2018**, *44*, 460–489. [[CrossRef](#)]
40. Arenillas, I.; Arz, J.A.; Molina, E.; Dupuis, C. An independent test of planktonic foraminiferal turnover across the Cretaceous/Paleogene (K/P) boundary at El Kef, Tunisia: Catastrophic mass extinction and possible survivorship. *Micropaleontology* **2000**, *46*, 31–49.
41. Arenillas, I.; Arz, J.A.; Molina, E.; Dupuis, C. The Cretaceous/Paleogene (K/P) boundary at Ain Settara, Tunisia: Sudden catastrophic mass extinction in planktic foraminifera. *J. Foraminifer. Res.* **2000**, *30*, 202–218. [[CrossRef](#)]
42. Alegret, L.; Arenillas, I.; Arz, J.A.; Molina, E. Foraminiferal event-stratigraphy across the Cretaceous/Tertiary boundary. *Neues Jahrb. Geol. Paläontol. Abh.* **2004**, *234*, 25–50. [[CrossRef](#)]
43. Arz, J.A.; Arenillas, I.; Molina, E.; Dupuis, C. Los efectos tafonómico y “Signor-Lipps” sobre la extinción en masa de foraminíferos planctónicos en el límite Cretácico/Terciario de Elles (Tunicia). *Rev. Soc. Geol. Esp.* **1999**, *12*, 251–268.
44. Arz, J.A.; Arenillas, I.; Grajales-Nishimura, J.M.; Liesa, C.; Soria, A.R.; Rojas-Consuegra, R.; Calmus, T.; Gilabert, V. No evidence of multiple impact scenario across the K/Pg boundary based on planktic foraminiferal biochronology. In *From the Guajira Desert to the Apennines, and from Mediterranean Microplates to the Mexican Killer Asteroid: Honoring the Career of Walter*; Geological Society of America Special Paper 557; Koerber, C., Claeys, P., Montanari, A., Eds.; Geological Society of America: Boulder, CO, USA, 2022; in press.
45. Arenillas, I.; Arz, J.A.; Grajales-Nishimura, J.M.; Murillo-Muñetón, G.; Alvarez, W.; Camargo-Zanoguera, A.; Molina, E.; Rosales-Domínguez, C. Chicxulub impact event is Cretaceous/Paleogene boundary in age: New micropaleontological evidence. *Earth Planet. Sci. Lett.* **2006**, *249*, 241–257. [[CrossRef](#)]
46. Arenillas, I.; Arz, J.A.; Grajales-Nishimura, J.M.; Rojas-Consuegra, R. The Chicxulub impact is synchronous with the planktonic foraminifera mass extinction at the Cretaceous/Paleogene boundary: New evidence from the Moncada section, Cuba. *Geol. Acta* **2016**, *14*, 35–51.
47. Schulte, P.; Alegret, L.; Arenillas, I.; Arz, J.A.; Barton, P.J.; Bown, P.R.; Bralower, T.J.; Christeson, G.L.; Claeys, P.; Cockell, C.S.; et al. Response-Cretaceous Extinctions. *Science* **2010**, *328*, 975–976. [[CrossRef](#)]
48. Chacón, B.; Martín-Chivelet, J. Subdivisión litoestratigráfica de las series hemipelágicas de edad Coniaciense-Thanetiense en el Prebético oriental (SE de España). *Rev. Soc. Geol. Esp.* **2005**, *18*, 3–20.
49. Smit, J. The section of the Barranco del Gredero (Caravaca, SE Spain): A crucial section for the Cretaceous/Tertiary boundary impact extinction hypothesis. *J. Iberian Geol.* **2004**, *31*, 179–191.
50. Martínez-Ruiz, F.; Ortega-Huertas, M.; Palomo-Delgado, I.; Barbieri, M. The geochemistry and mineralogy of the Cretaceous-Tertiary boundary at Agost (southeast Spain). *Chem. Geol.* **1992**, *95*, 265–281. [[CrossRef](#)]

51. Martínez-Ruiz, F.; Ortega-Huertas, M.; Palomo-Delgado, I.; Acquafredda, P. Quench textures in altered spherules from the Cretaceous-Tertiary boundary layer at Agost and Caravaca, SE Spain. *Sediment. Geol.* **1997**, *113*, 137–147. [[CrossRef](#)]
52. Kaiho, K.; Kajiwara, Y.; Tazaki, K.; Ueshima, M.; Takeda, N.; Kawahata, H.; Arinobu, T.; Ishiwatari, R.; Hirai, A.; Lamolda, M.A. Oceanic primary productivity and dissolved oxygen levels at the Cretaceous/Tertiary Boundary: Their decrease, subsequent warming, and recovery. *Paleoceanography* **1999**, *14*, 511–524. [[CrossRef](#)]
53. Canudo, J.I.; Keller, G.; Molina, E. Cretaceous/Tertiary boundary extinction pattern and faunal turnover at Agost and Caravaca, SE Spain. *Mar. Micropaleontol.* **1991**, *17*, 319–341. [[CrossRef](#)]
54. Gradstein, F.M.; Ogg, J.G.; Schmitz, M.D.; Ogg, G.M. *The Geologic Time Scale 2020*; Elsevier: Amsterdam, The Netherlands, 2020; p. 1357.
55. Dinarès-Turell, J.; Westerhold, T.; Pujalte, V.; Röhl, U.; Kroon, D. Astronomical calibration of the Danian stage (Early Paleocene) revisited: Settling chronologies of sedimentary records across the Atlantic and Pacific Oceans. *Earth Planet. Sci. Lett.* **2014**, *405*, 119–131. [[CrossRef](#)]
56. Mukhopadhyay, S.; Farley, K.A.; Montanari, A. A short duration of the Cretaceous-Tertiary boundary event: Evidence from extraterrestrial Helium-3. *Science* **2001**, *291*, 1952–1955. [[CrossRef](#)]
57. Groot, J.J.; de Jonge, R.B.G.; Langereis, C.G.; Ten Kate, W.G.H.Z.; Smit, J. Magnetostratigraphy of the Cretaceous-Tertiary boundary at Agost (Spain). *Earth Planet. Sci. Lett.* **1989**, *94*, 385–397. [[CrossRef](#)]
58. Margolis, S.V.; Mount, J.F.; Doehne, E.; Showers, W.J. The Cretaceous/Tertiary Boundary Carbon and Oxygen Isotope Stratigraphy, Diagenesis, and Paleoceanography at Zumaya, Spain. *Paleoceanogr. Paleoeclimatol.* **1987**, *2*, 361–377. [[CrossRef](#)]
59. Smit, J. Meteorite impact, extinctions and the Cretaceous-Tertiary boundary. *Geol. Mijnbouw* **1990**, *69*, 187–204.
60. Ortega-Huertas, M.; Martínez-Ruiz, F.; Palomo, I.; Chamley, H. Comparative mineralogical and geochemical clay sedimentation in the Betic Cordilleras and Basque-Cantabrian Basin areas at the Cretaceous-Tertiary boundary. *Sediment. Geol.* **1995**, *94*, 209–227. [[CrossRef](#)]
61. Ten Kate, W.G.H.Z.; Sprenger, A. Orbital cyclicities above and below the Cretaceous/Paleogene boundary at Zumaya (N Spain), Agost and Relleu (SE Spain). *Sediment. Geol.* **1993**, *87*, 69–101. [[CrossRef](#)]
62. Dinarès-Turell, J.; Baceta, J.I.; Pujalte, V.; Orue-Etxebarria, X.; Bernaola, G.; Lorito, S. Untangling the Palaeocene climatic rhythm: An astronomically calibrated Early Palaeocene magnetostratigraphy and biostratigraphy at Zumaia (Basque basin, northern Spain). *Earth Planet. Sci. Lett.* **2003**, *216*, 483–500. [[CrossRef](#)]
63. Kuiper, K.F.; Deino, A.; Hilgen, F.J.; Krijgsman, W.; Renne, P.R.; Wijbrans, J.R. Synchronizing rock clocks of earth history. *Science* **2008**, *320*, 500–504. [[CrossRef](#)]
64. Westerhold, T.; Röhl, U.; Raffi, I.; Fornaciari, E.; Monechi, S.; Reale, V.; Bowles, J.; Evans, H.F. Astronomical calibration of the Paleocene time. *Palaeogeogr. Palaeoclimatol. Palaeoecol.* **2008**, *257*, 377–403. [[CrossRef](#)]
65. Hilgen, F.J.; Kuiper, K.F.; Lourens, L.J. Evaluation of the astronomical time scale for the Paleocene and earliest Eocene. *Earth Planet. Sci. Lett.* **2010**, *300*, 139–151. [[CrossRef](#)]
66. Hilgen, F.J.; Abels, H.A.; Kuiper, K.F.; Lourens, L.J.; Wolthers, M. Towards a stable astronomical time scale for the Paleocene: Aligning Shatsky Rise with the Zumaia–Walvis Ridge ODP site 1262 composite. *Newsl. Stratigr.* **2015**, *48*, 91–110. [[CrossRef](#)]
67. Batenburg, S.J.; Sprovieri, M.; Gale, A.; Hilgen, F.J.; Hüsing, S.; Laskar, J.; Liebrand, D.; Lirer, F.; Orue-Etxebarria, X.; Pelosi, N.; et al. Cyclostratigraphy and astronomical tuning of the Late Maastrichtian at Zumaia (Basque country, Northern Spain). *Earth Planet. Sci. Lett.* **2012**, *359–360*, 264–278. [[CrossRef](#)]
68. Batenburg, S.J.; Gale, A.; Sprovieri, M.; Hilgen, F.J.; Thibault, N.; Boussaha, M.; Orue-Etxebarria, X. An astronomical time scale for the Maastrichtian based on the Zumaia and Sopelana sections (Basque country, northern Spain). *J. Geol. Soc. Lond.* **2014**, *171*, 165–180. [[CrossRef](#)]
69. Laskar, J.; Gastineau, M.; Delisle, J.-B.; Farrés, A.; Fienga, A. Strong chaos induced by close encounters with Ceres and Vesta. *Astron. Astrophys.* **2011**, *532*, 4. [[CrossRef](#)]
70. Schoene, B.; Eddy, M.P.; Samperton, K.M.; Keller, C.B.; Keller, G.; Adatte, T.; Khadri, S.F.R. U-Pb constraints on pulsed eruption of the Deccan Traps across the end-Cretaceous mass extinction. *Science* **2019**, *363*, 862–866. [[CrossRef](#)]
71. Sprain, C.J.; Renne, P.R.; Clemens, W.A.; Wilson, G.P. Calibration of chron C29r: New high-precision geochronologic and paleomagnetic constraints from the Hell Creek region, Montana. *Bull. Geol. Soc. Am.* **2018**, *130*, 1615–1644. [[CrossRef](#)]
72. Asgharian Rostami, M.; Leckie, R.M.; Font, E.; Frontalini, F.; Finkelstein, D.; Koeberl, C. The Cretaceous-Paleogene transition at Galanderud (northern Alborz, Iran): A multidisciplinary approach. *Palaeogeogr. Palaeoclimatol. Palaeoecol.* **2018**, *493*, 82–101. [[CrossRef](#)]
73. Coccioni, R.; Frontalini, F.; Bancalà, G.; Fornaciari, E.; Jovane, L.; Sprovieri, M. The Dan-C2 hyperthermal event at Gubbio (Italy): Global implications, environmental effects, and cause(s). *Earth Planet. Sci. Lett.* **2010**, *297*, 298–305. [[CrossRef](#)]
74. Lowery, C.M.; Jones, H.L.; Bralower, T.; Pérez-Cruz, L.; Gebhardt, C.; Whalen, M.T.; Chenot, E.; Smit, J.; Phillips, M.P.; Choumiline, K.; et al. Early Paleocene paleoceanography and export productivity in the Chicxulub Crater. *Paleoceanogr. Paleoeclimatol.* **2021**, *36*, e2021PA004241. [[CrossRef](#)]
75. Gallala, N.; Zaghbib-Turki, D.; Molina, E.; Arenillas, I.; Arz, J.A. Catastrophic mass extinction and assemblage evolution in planktic foraminiferal across the Cretaceous/Paleogene (K/Pg) boundary at Bidart (SW France). *Mar. Micropaleontol.* **2009**, *72*, 196–209. [[CrossRef](#)]

76. D'Hondt, S.; Keller, G. Some patterns of planktic foraminiferal assemblage turnover at the Cretaceous-Tertiary boundary. *Mar. Micropaleontol.* **1991**, *17*, 77–118. [[CrossRef](#)]
77. Apellaniz, E.; Baceta, J.I.; Bernaola-Bilbao, G.; Núñez-Betelu, K.; Orue-Etxebarria, X.; Payros, A.; Pujalte, V.; Robin, E.; Rocchia, R. Analysis of uppermost Cretaceous-lowermost Tertiary hemipelagic successions in the Basque Country (Western Pyrenees): Evidence for a sudden extinction of more than half planktic foraminifer species at the K/T boundary. *Bull. Soc. Géol. France* **1997**, *168*, 783–793.
78. Birch, H.S.; Coxall, H.C.; Pearson, P.N.; Kroon, D.; Schmidt, D.N. Partial collapse of the marine carbon pump after the Cretaceous–Paleogene boundary. *Geology* **2016**, *44*, 287–290. [[CrossRef](#)]
79. Aze, T.; Ezard, T.H.G.; Purvis, A.; Coxall, H.; Stewart, D.R.M.; Wade, B.S.; Pearson, P.N. A phylogeny of Cenozoic macroperforate planktonic foraminifera from fossil data. *Biol. Rev.* **2011**, *86*, 900–927. [[CrossRef](#)]
80. Huber, B.T. Evidence for planktonic foraminifer reworking versus survivorship across the Cretaceous–Tertiary boundary at high latitudes. *Geol. Soc. Am. S. Pap.* **1996**, *307*, 319–334. [[CrossRef](#)]
81. Smit, J.; Nederbragt, A.J. Analysis of the El Kef blind test II. *Mar. Micropaleontol.* **1997**, *29*, 95–100. [[CrossRef](#)]
82. Kaiho, K.; Lamolda, M.A. Catastrophic extinction of planktonic foraminifera at the Cretaceous-Tertiary boundary evidenced by stable isotopes and foraminiferal abundance at Caravaca, Spain. *Geology* **1999**, *27*, 355–358. [[CrossRef](#)]
83. Huber, B.T.; MacLeod, K.G.; Norris, R. Abrupt extinction and subsequent reworking of Cretaceous planktonic foraminifera across the Cretaceous/Tertiary boundary: Evidence for the subtropical North Atlantic. *Geol. Soc. Am.* **2002**, *356*, 277–290. [[CrossRef](#)]
84. Herm, D.; Von Hillebrandt, A.; Perch-Nielsen, K. Die Kreide/Tertiär-Grenze im Lattengebirge (Nördliche Kalkalpen) in mikropaläontologischer Sicht. *Geol. Bavarica* **1981**, *82*, 319–344.
85. Premoli Silva, I.; Bolli, H.M. Late Cretaceous to Eocene planktonic foraminifera and stratigraphy of Leg 15 sites in the Caribbean Sea. *Initial Rep. Deep Sea Drill. Proj.* **1973**, *15*, 449–547. [[CrossRef](#)]
86. Canudo, J.I.; Molina, E. Bioestratigrafía con foraminíferos planctónicos del Paleógeno del Pirineo. *Neues Jahrb. Geol. Paläontol. Abh.* **1992**, *186*, 97–135.
87. Luciani, V. Planktonic foraminiferal turnover across the Cretaceous-Tertiary boundary in the Vajont valley (Southern Alps, northern Italy). *Cretac. Res.* **1997**, *18*, 799–821. [[CrossRef](#)]
88. Morozova, V.G. Stratigrafiya Datsko-Montskikh otlozhenii Kryma po foraminiferam Stratigraphy of the Danian-Montian deposits of the Crimea according to the foraminifera. *Dokl. Akad. Nauk SSSR* **1959**, *124*, 1113–1116.
89. Morozova, V.G. Zonal'naya stratigrafiya Datsko-Monstkikh otlozhenii CCCR i granitsa mela c paleogenom Stratigraphical zonation of the Danish-Montian deposits of the USSR and the Cretaceous-Paleogene boundary. In *Problema V: Granitsa Melovoi i Paleogenovoi Sistem. Mezhdunarodnyi Geologicheskii Kongress; XXI Sessiya, Doklady Sovetskikh Geologov, Izdatelstvo Akademiya Nauk SSR; Academy of Science of the Union of Soviet Socialist Republics: Moscow, Union of Soviet Socialist Republics, 1960; pp. 83–100.*
90. Keller, G.; Adatte, T.; Stinnesbeck, W.; Luciani, V.; Karoui-Yaakoub, N.; Zaghbib-Turkie, D. Paleoecology of the Cretaceous–Tertiary mass extinction in planktonic foraminifera. *Palaeogeogr. Palaeoclimatol. Palaeoecol.* **2002**, *178*, 257–297. [[CrossRef](#)]
91. Luciani, V. High-resolution planktonic foraminiferal analysis from the Cretaceous–Tertiary boundary at Ain Settara (Tunisia): Evidence of an extended mass extinction. *Palaeogeogr. Palaeoclimatol. Palaeoecol.* **2002**, *178*, 299–319. [[CrossRef](#)]
92. Coccioni, R.; Luciani, V. Guembelitra irregularis bloom at the K-T boundary: Morphological abnormalities induced by impact-related extreme environmental stress? In *Biological Processes Associated with Impact Events; Cockell, C., Gilmour, I., Koeberl, C., Eds.; Springer: Berlin/Heidelberg, Germany, 2006; pp. 179–196.*
93. Brinkhuis, H.; Zachariasse, W.J. Dinoflagellate cysts, sea level changes and planktonic foraminifers across the Cretaceous-Tertiary boundary at El Haria, Northwest Tunisia. *Mar. Micropaleontol.* **1988**, *13*, 153–191. [[CrossRef](#)]